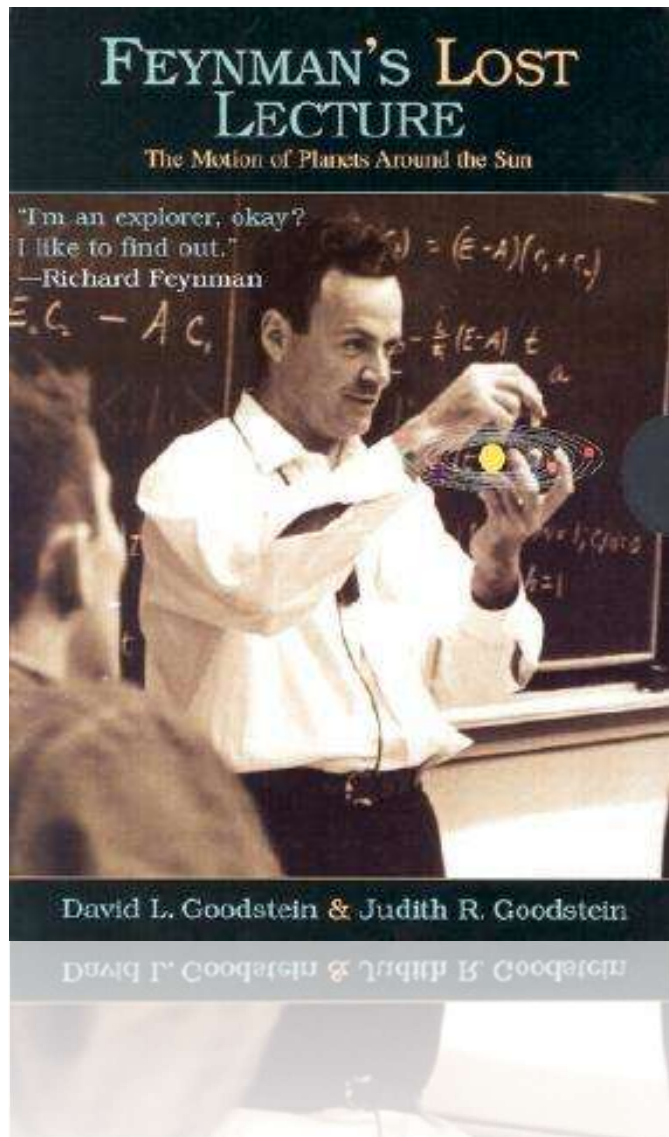


Lecture-9

CSO202: Atoms, Photons & Molecules

Debabrata Goswami



elementary
Simple things have simple
demonstrations

You can explain to people who don't know much of the physics, the early history... how Newton discovered... Kepler's Laws, and equal areas, and that means it's toward the sun, and all this stuff. And then the key - they always ask then, "Well, how do you see that it's an ellipse if it's the inverse square?" Well, it's God damned hard, there's no question of that. But I tried to find the simplest one I could.

teacher

The problem facing the ~~scientist~~ has been compared with that of a spectator of a drastically shortened version of a classical drama -

"Hamlet" say - where he or she is only shown the opening scenes of the first act and the last scene of the finale. The main characters are introduced, then the curtain falls for change of scenery and as it rises again we see on the scene floor a considerable number of "dead" bodies and a few survivors. Not an easy task for the inexperienced to unravel what actually took place in between.

Atoms, Photons & Molecules

Objective

Convey the excitement of modern physical chemistry through presenting and analyzing some of the key experiments. What concepts are needed to understand the experiments and their impact?

1. Interplay of experiment and theory.
 2. Diversity of chemical reactions - gas phase, on surfaces, and in solutions.
 3. Timescales, length scales, and energetics.
-

Module 1, Part A:

**Chemical Reaction through Collision Dynamics of
Reactants to Produce Products**

Elementary chemical reactions



Dudley R.
Herschbach



Yuan T. Lee



John C.
Polanyi

The Nobel Prize in Chemistry 1986



The Official Web Site of the Nobel Prize

$$E_v = \tilde{\nu} \left(v + \frac{1}{2} \right) - \tilde{x} \tilde{\nu} \left(v + \frac{1}{2} \right)^2$$

Energy & momentum conservation

rebounding
vs
stripping

Experiment

Classical

Quantum
Forward

backwards

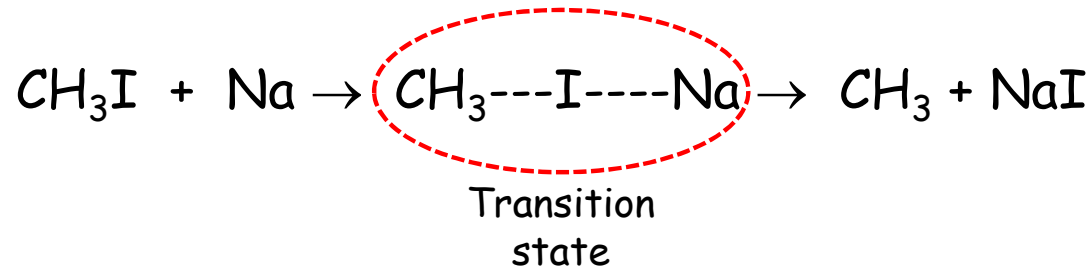
Molecular beams

$$E_c = \frac{1}{2} \mu v^2$$

Module 1, Part B:

Ultrafast Chemical Reaction Dynamics with Ultrashort-Pulsed Lasers

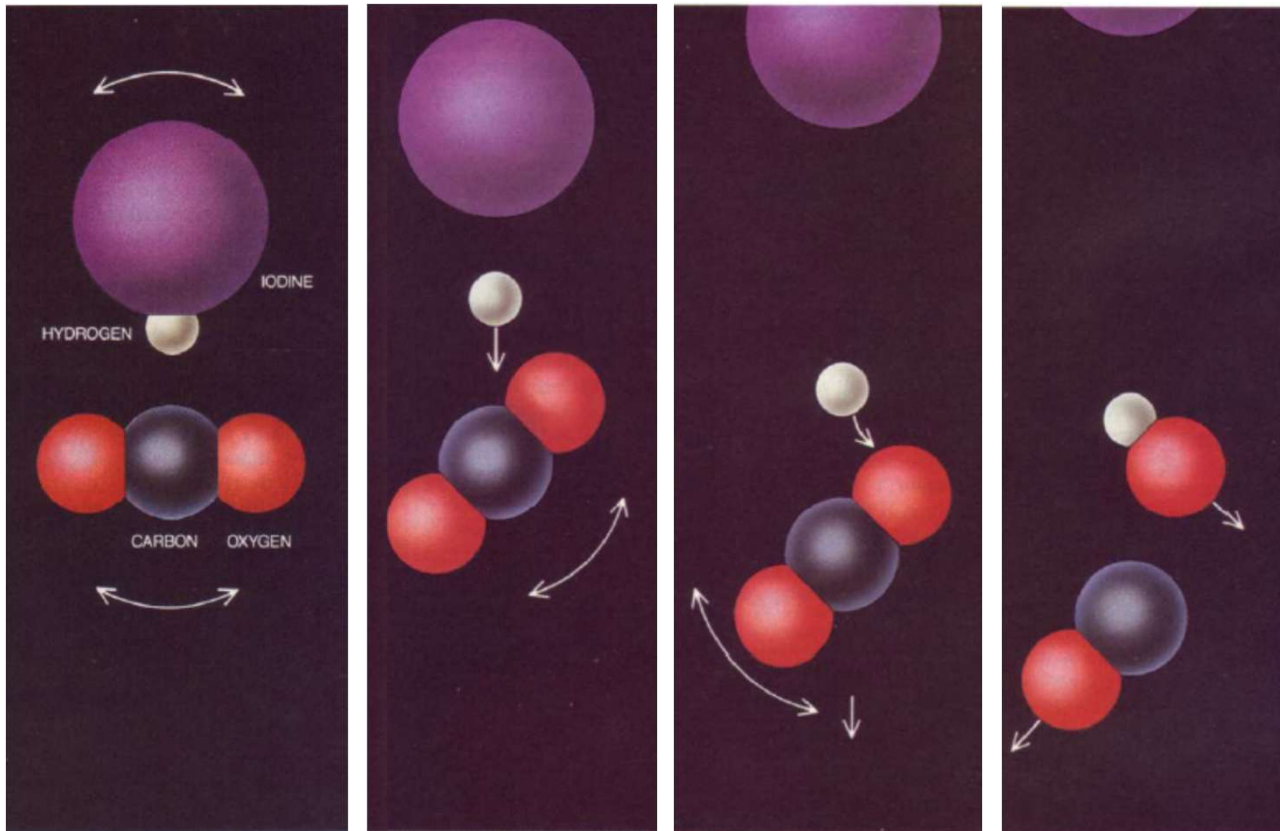
Consider a chemical transformation



In any chemical reaction the motions of the electrons and nuclei of atoms determine how the molecules interact, and those interactions in turn create the forces that govern the reaction's dynamics.

If one can determine how molecular motions change during the critical transition phase, we can understand how new chemical bonds form and old ones disappear.

CSO 202A : Atoms Molecules and Photons



Molecular structures for a reaction in progress involving two molecules (bimolecular).

Question

How can one study transition state(s) in real time?

Answer

Need ultrafast probe and detection technique

Measuring the immeasurable!



Ahmed H.
Zewail

FEMTOCHEMISTRY

ATOMIC-SCALE DYNAMICS OF THE CHEMICAL BOND
USING ULTRAFAST LASERS

Nobel Lecture, December 8, 1999

by

AHMED H. ZEWAIL

California Institute of Technology, Pasadena, USA.

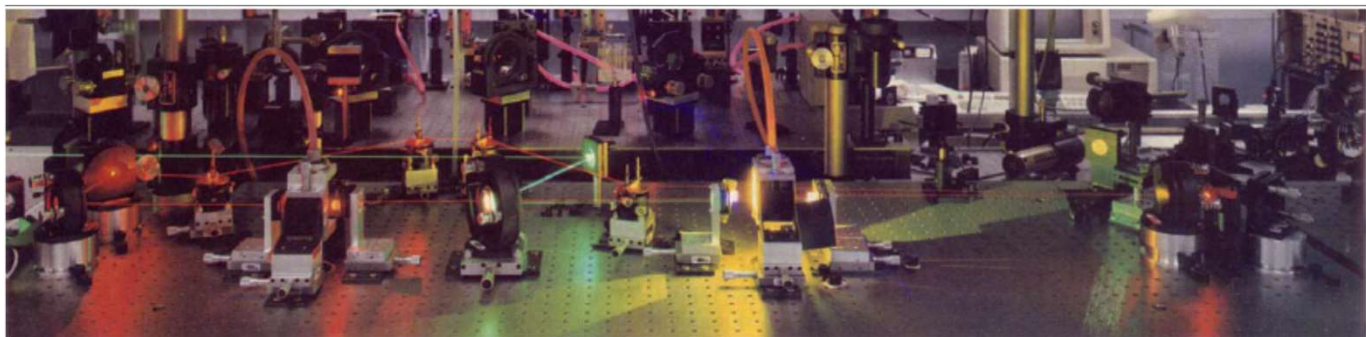
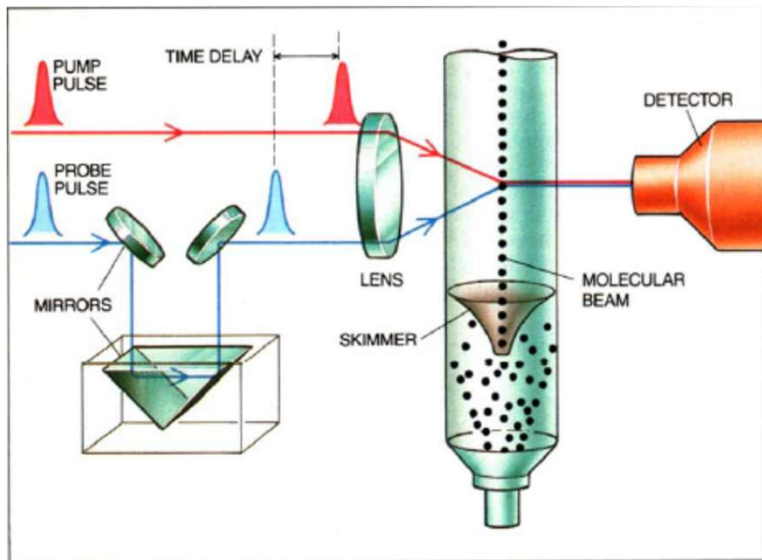
The Nobel Prize in Chemistry 1999



Nobelprize.org

The Official Web Site of the Nobel Prize

CSO 202 : Atoms Molecules and Photons



J. Chem. Phys., 1987, 87(4), 2395

Real-time femtosecond probing of “transition states” in chemical reactions^{a)}

Marcos Dantus, Mark J. Rosker, and Ahmed H. Zewail^{b)}

Arthur Amos Noyes Laboratory of Chemical Physics,^{c)} California Institute of Technology, Pasadena, California 91125

(Received 3 June 1987; accepted 15 June 1987)

Transition state(s) (TS) of chemical reactions are fundamental in defining the region(s) of internuclear separation (R^*) on the potential energy surface (PES) at which the reagent molecule is “passing on” to products.¹ In contrast to the many successes in applying spectroscopies to the characterization of *stable* reagents and *stable* products, TS spectroscopy has been very limited, because of the TS ultra-short lifetime (few vibrational periods) and the very low

density of TS molecules that can be probed at R^* . Recently, elegant ideas of time-integrated emission,² absorption,³ and scattering⁴ spectroscopy have been developed to infer the dynamics of the TS. Here, we offer a real-time technique that, because of its time resolution (~ 40 fs), promises to provide direct information concerning the TS and the spectroscopy of reaction intermediates in the process of falling apart (dissociation) or forming a chemical bond (associ-

CSO 202 : Atoms Molecules and Photons

Femtosecond real-time probing of reactions. I. The technique

Mark J. Rosker, Marcos Dantus, and Ahmed H. Zewail^{a)}

*Arthur Amos Noyes Laboratory of Chemical Physics, California Institute of Technology, Pasadena,
California 91125*

(Received 12 July 1988; accepted 11 August 1988)

When a chemical bond is broken in a direct dissociation reaction, the process is so rapid that it has generally been considered instantaneous and therefore unobservable. But the fragments formed interact with one another for times on the order of 10^{-13} s after the photon has been absorbed. On this time scale the system passes through intermediate transition configurations; the totality of such configurations have been, in the recent literature, designated as "transition states." Femtosecond transition-state spectroscopy (FTS) is a real-time technique for probing chemical reactions. It allows the direct observation of a molecule in the process of falling apart or in the process of formation. In this paper, the first in a series on femtosecond real-time probing of reactions, we examine the technique in detail. The concept of FTS is explored, and the interrelationship between the dynamics of chemical reactions and molecular potential energy surfaces is considered. The experimental method, which requires the generation of spectrally tunable femtosecond optical pulses, is detailed. Illustrative results from FTS experiments for several elementary reactions are presented, and we describe methods for relating these results to the potential energy surface(s).

J. Chem. Phys. 89 (10), 15 November 1988 0021-9606/88/226113-15\$02.10

© 1988 American Institute of Physics

6113

Femtosecond real-time probing of reactions. II. The dissociation reaction of ICN

Marcos Dantus, Mark J. Rosker, and Ahmed H. Zewail^{a)}

*Arthur Amos Noyes Laboratory of Chemical Physics, California Institute of Technology, Pasadena,
California 91125*

(Received 12 July 1988; accepted 11 August 1988)

Experimental results obtained for the dissociation reaction $\text{ICN}^* \rightarrow [\text{I} \cdots \text{CN}]^{**} \rightarrow \text{I} + \text{CN}$ using femtosecond transition-state spectroscopy (FTS) are presented. The process of the I-CN bond breaking is clocked, and the transition states of the reaction are observed in real time. From the clocking experiments, a "dissociation" time of 205 ± 30 fs was measured and was related to the length scale of the potential. The transition states live for only ~ 50 fs or less, and from the observed transients we deduce some characteristics of the relevant potential energy surfaces (PES). These FTS experiments are discussed in relation to both classical and quantum mechanical models of the dynamical motion, including features of the femtosecond coherence and alignment of fragments during recoil. The observations are related to the radial and angular properties of the PES.

6128

J. Chem. Phys. 89 (10), 15 November 1988 0021-9606/88/226128-13\$02.10

© 1988 American Institute of Physics

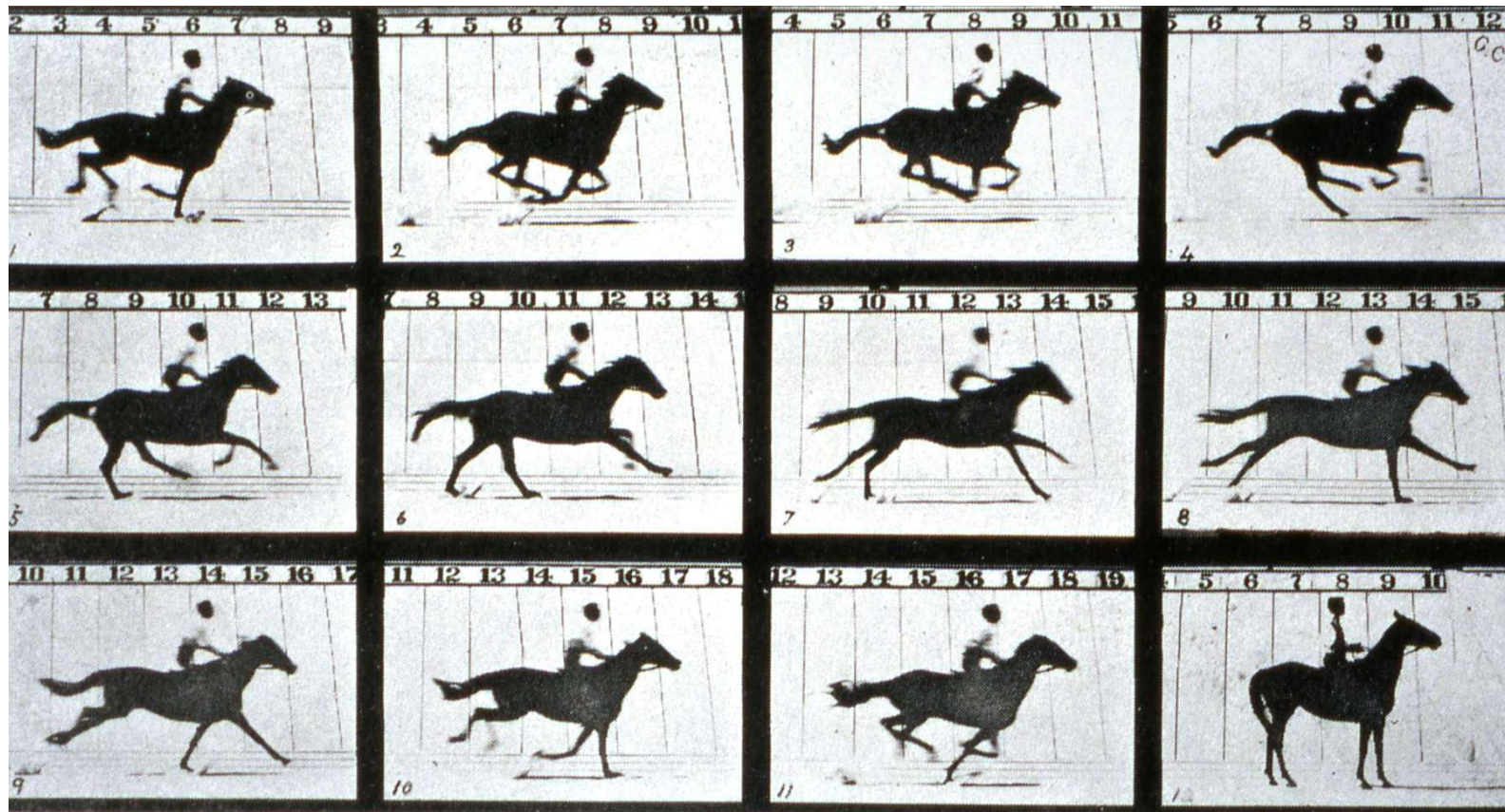
Trotting Horse

Movie



There was a debate over the question of whether all four hooves of a trotting horse are simultaneously out of contact with the ground at any point in its stride.

Eadweard Muybridge resolved this!



Time sequence
images of a
falling apple



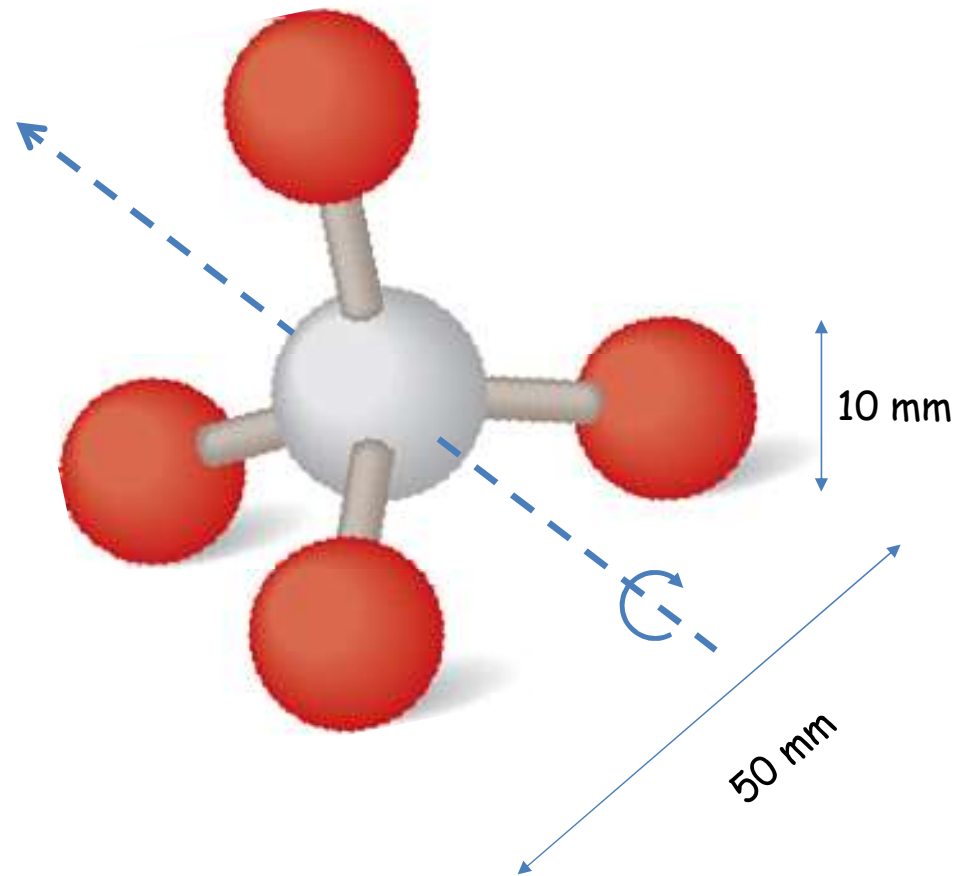
Q. How can you
get these time
sequence images?

A. Stroboscopy

What time
resolution is
needed to
capture sharp
images of the
falling apple????

Let's work it out

Let's take a molecular model, rotating at high speed (say -2600 rpm)



CSO 202 : Atoms Molecules and Photons

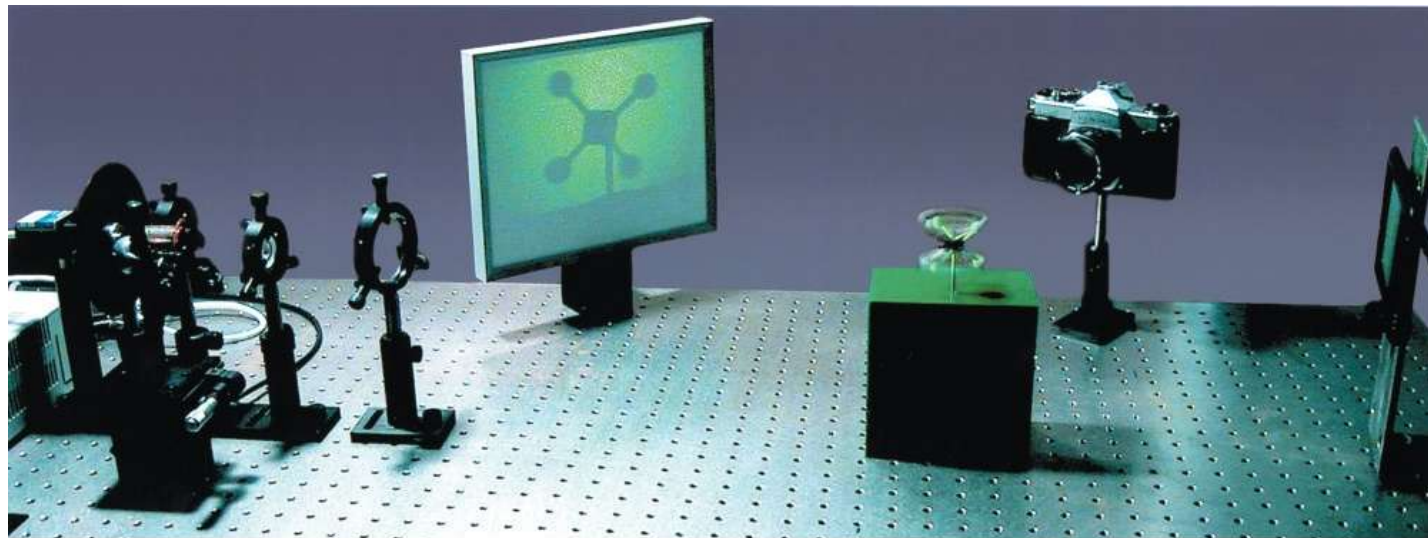
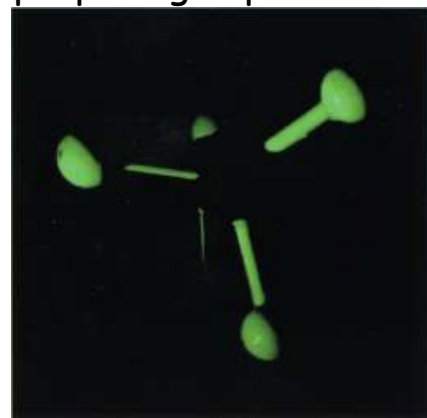
When static



View under room light
when rotating



Freezing motion using
proper light pulse

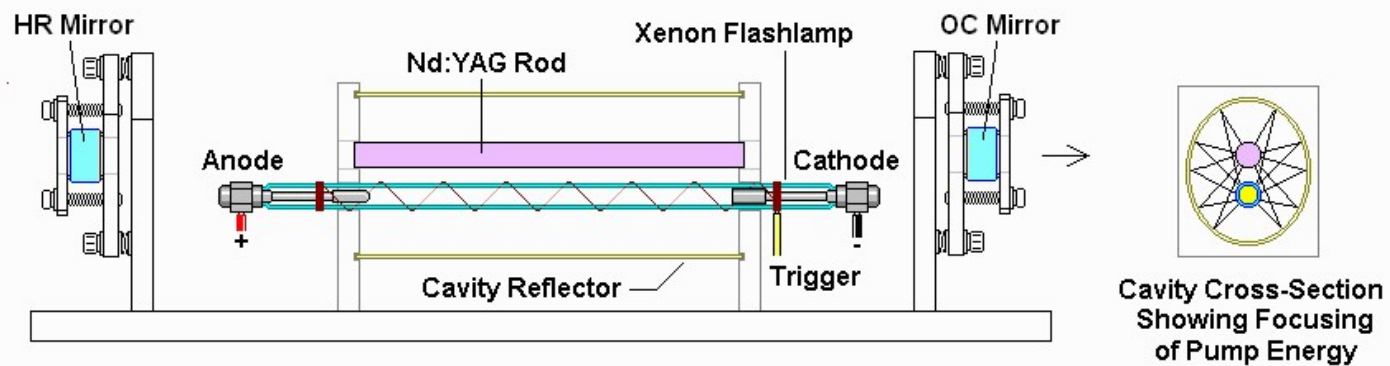


What time resolution is needed to freeze this macroscopic molecular model in motion???? Let's find it out → ~150 μ s !!! Need short pulse!

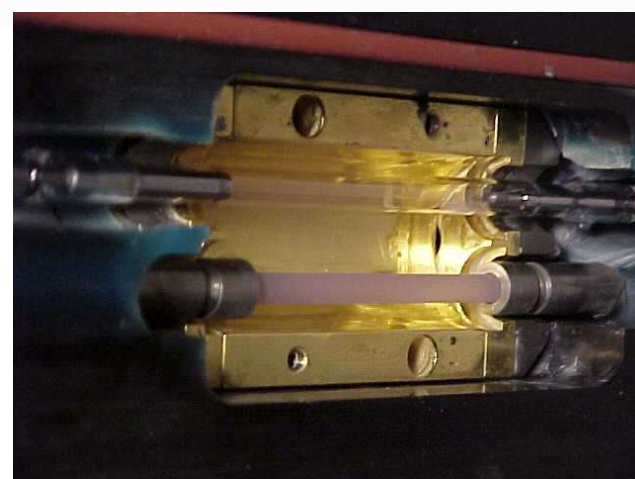
What about a real molecule (say methane)?
Let's work it out → ~10⁻¹² s !!! Need ultrashort pulse!

How can we generate light pulses???
Use Chopper. But, how to choose right parameters for the chopper???? Let's find out.

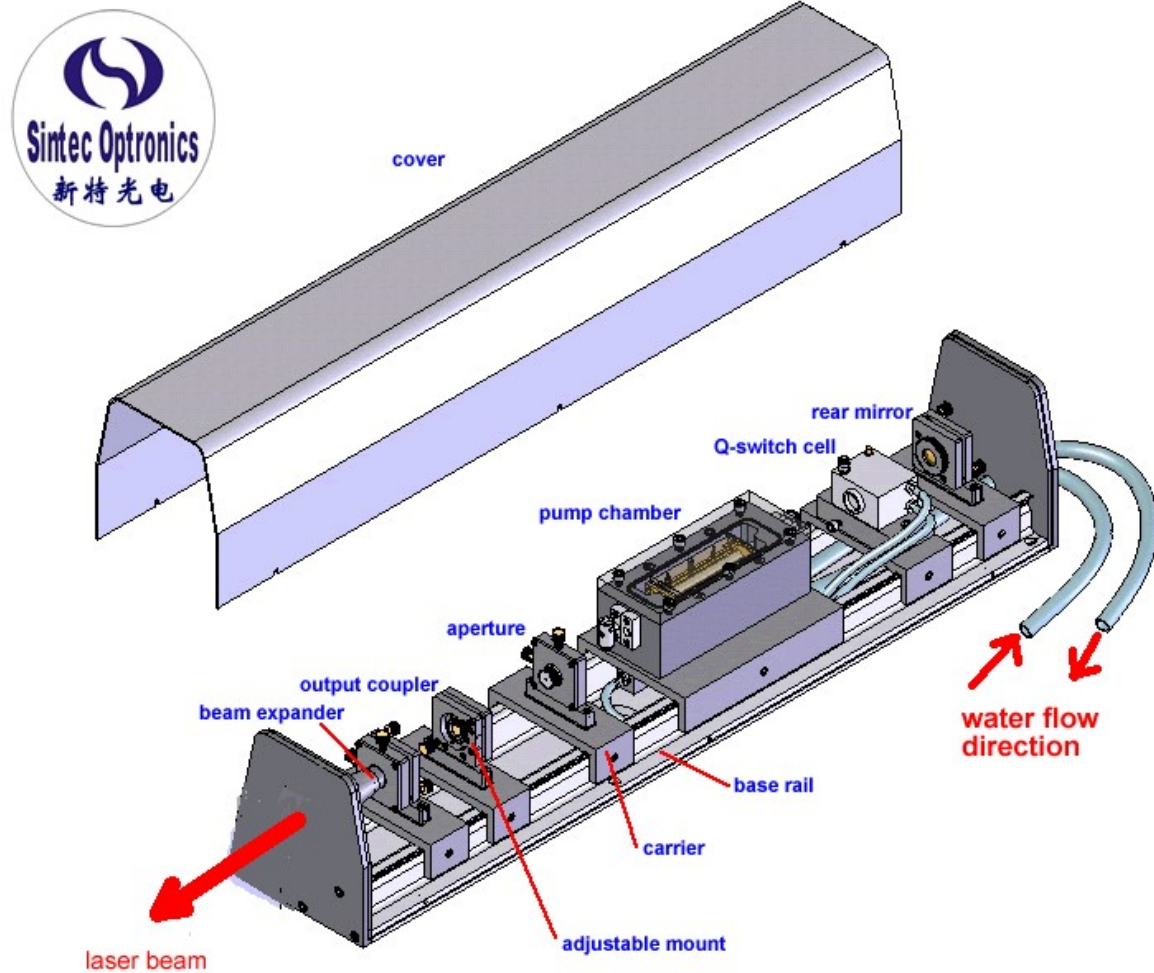
Is just achieving the time resolution good enough for our goal???
No. Need synchronization as well !! Why????



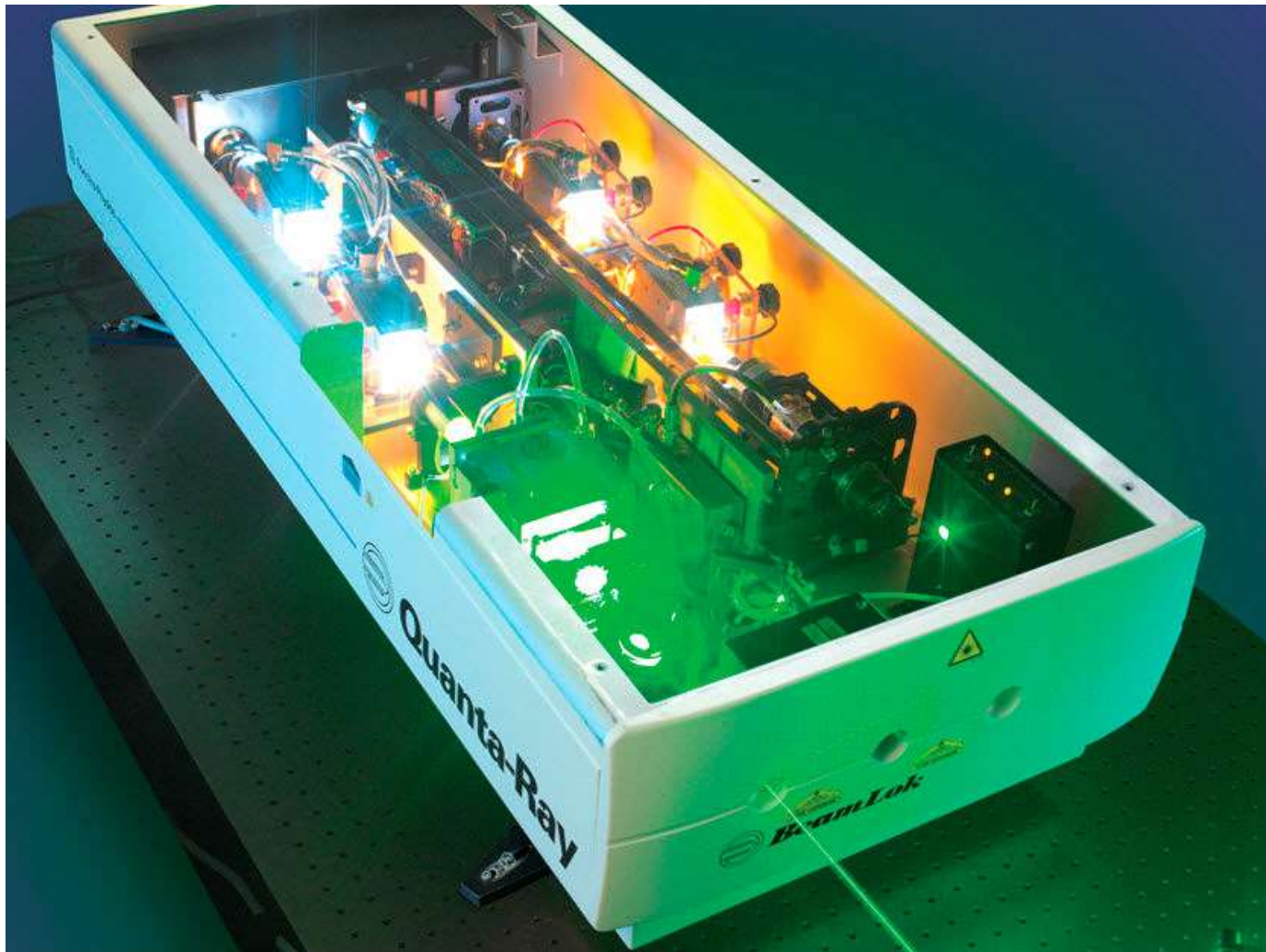
Pulsed Solid State Laser Assembly



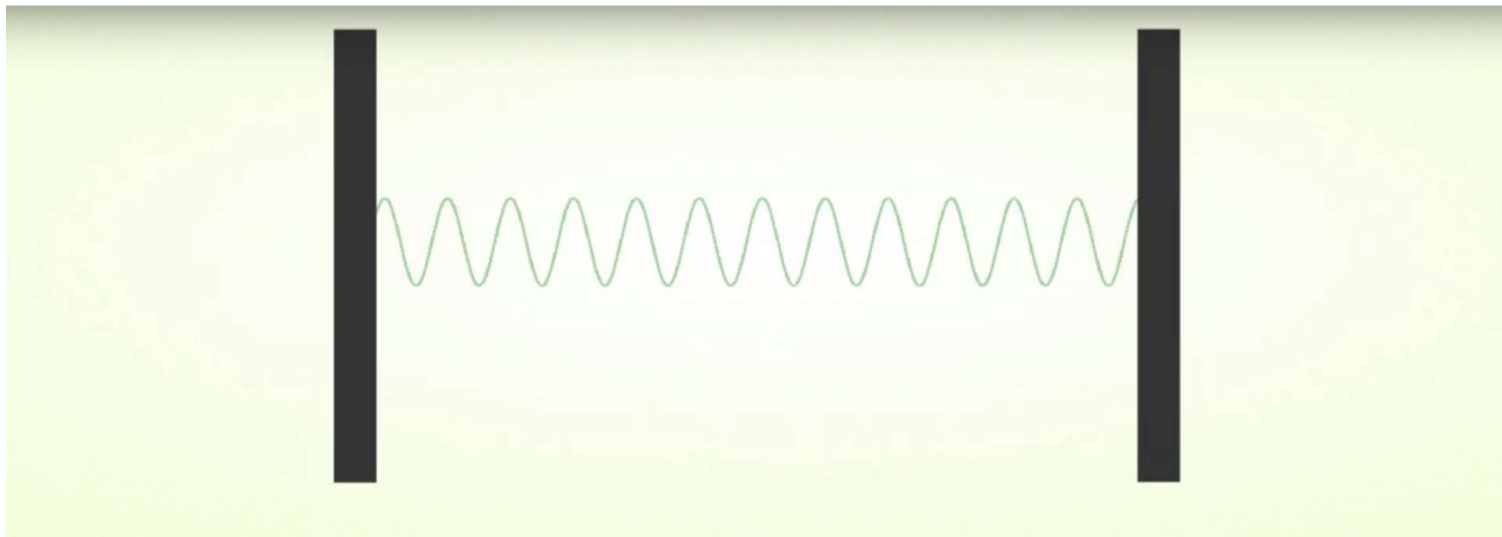
CSO 202 : Atoms Molecules and Photons



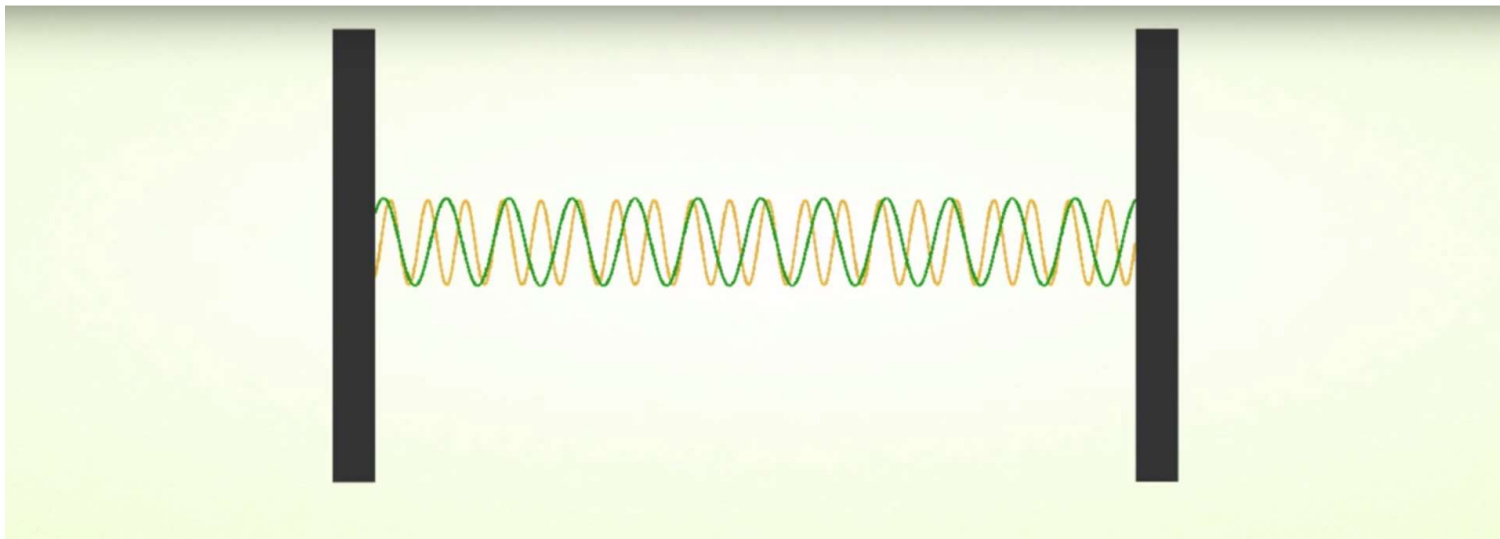
CSO 202 : Atoms Molecules and Photons



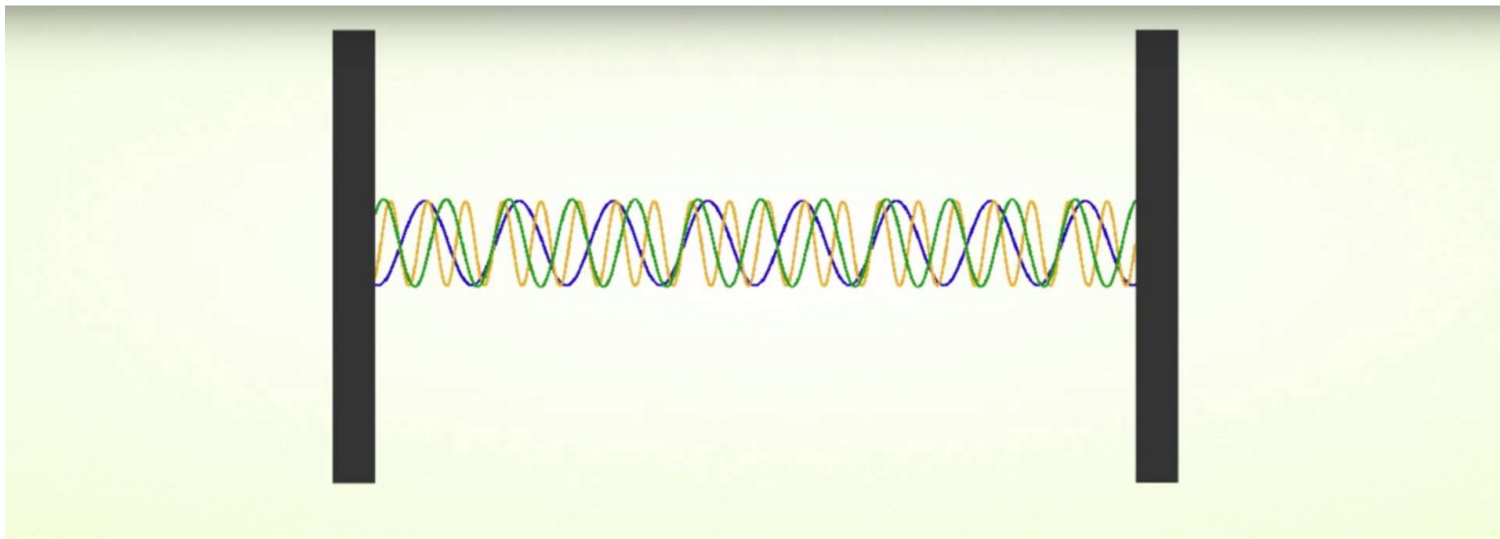
CSO 202 : Atoms Molecules and Photons



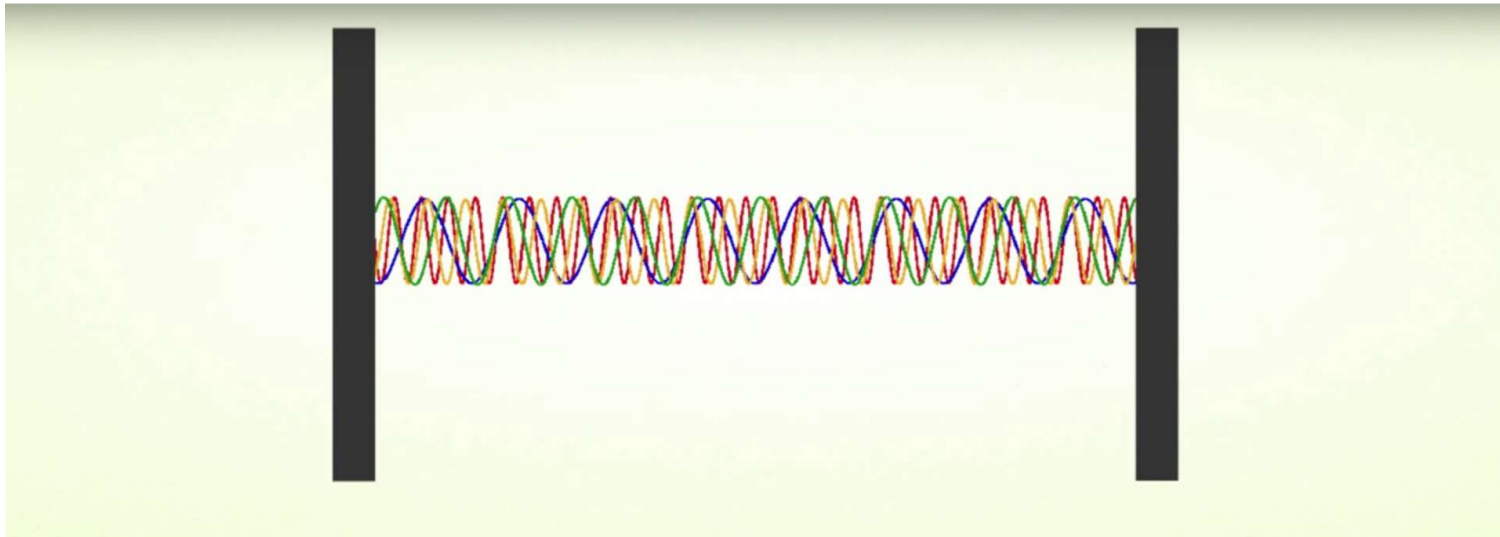
CSO 202 : Atoms Molecules and Photons

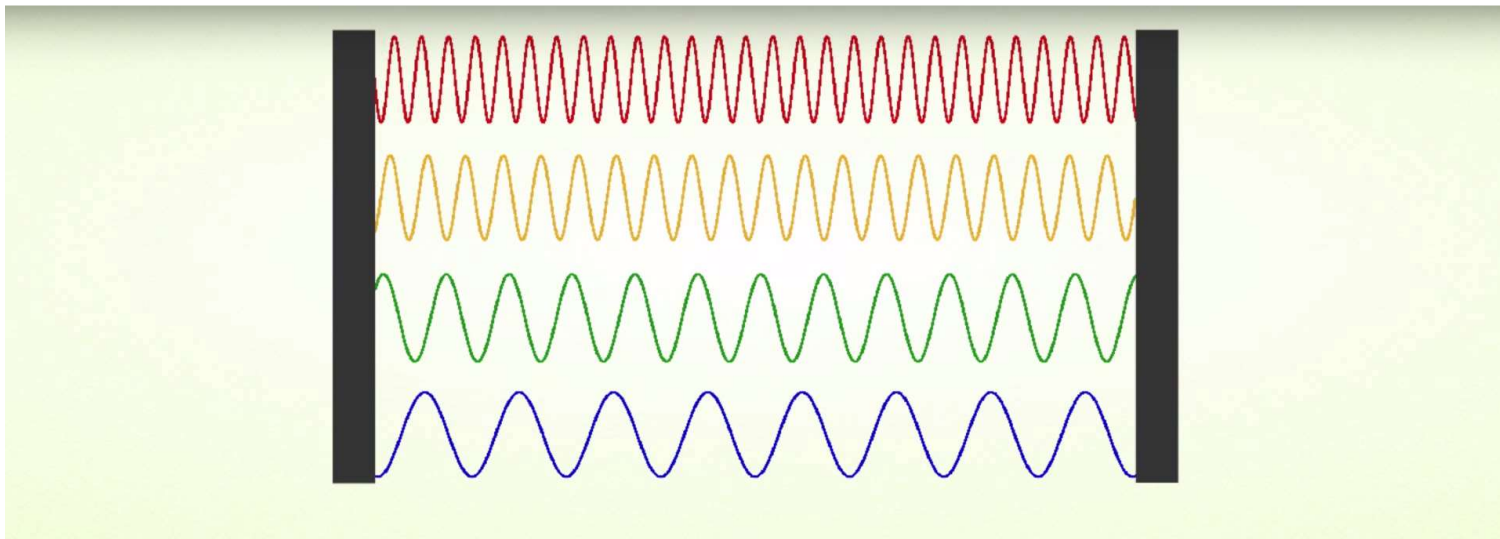


CSO 202 : Atoms Molecules and Photons

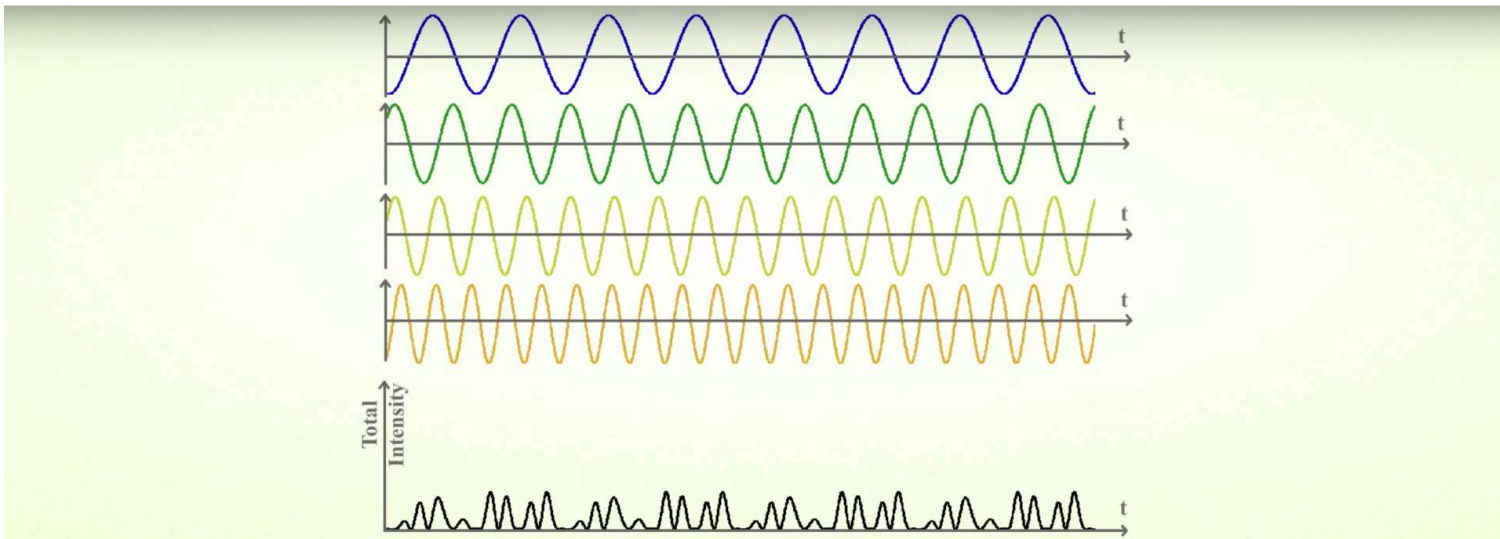


CSO 202 : Atoms Molecules and Photons

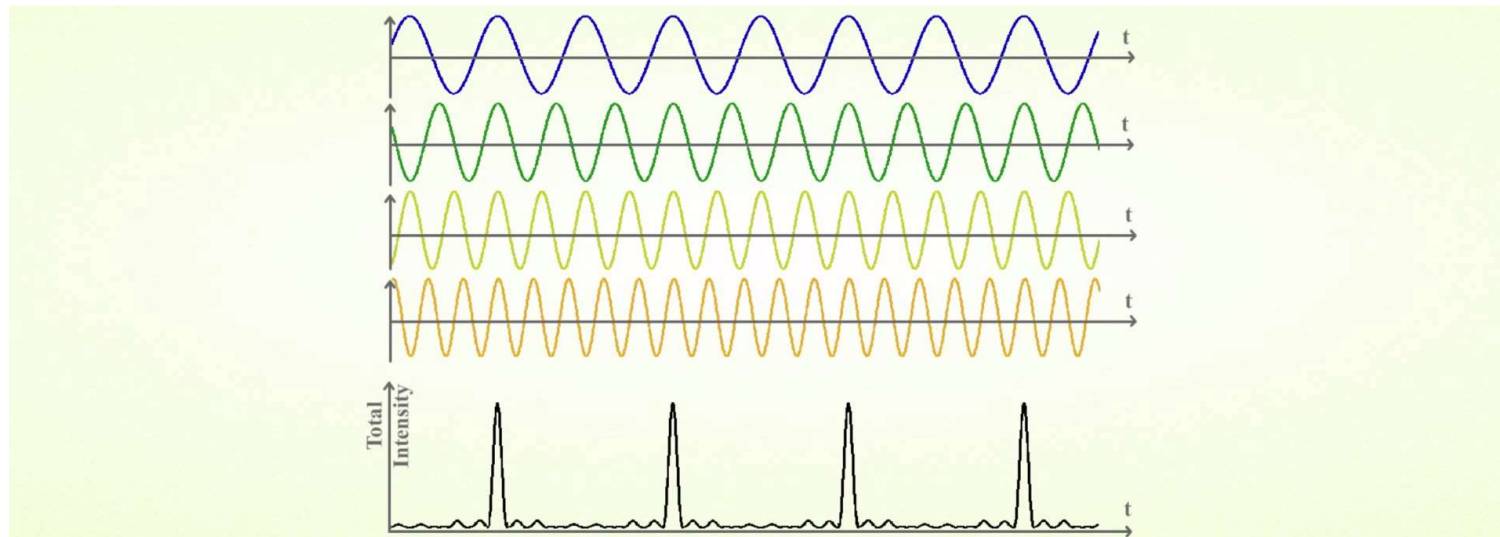




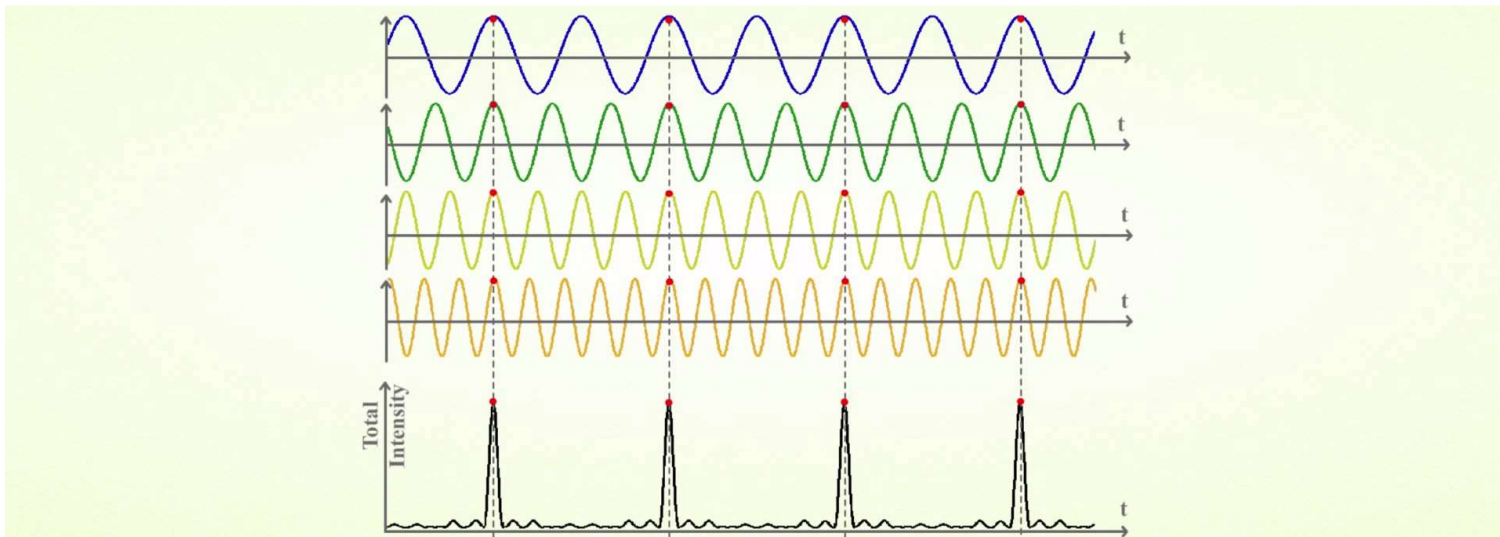
CSO 202 : Atoms Molecules and Photons

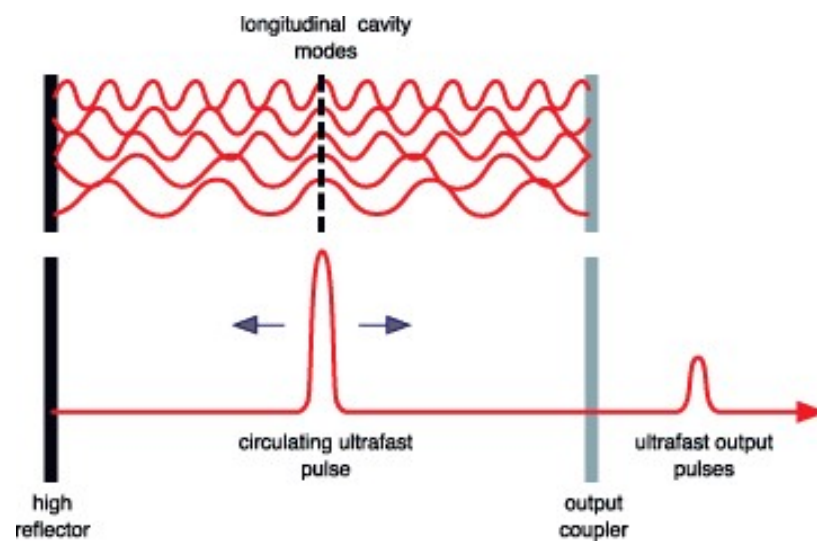


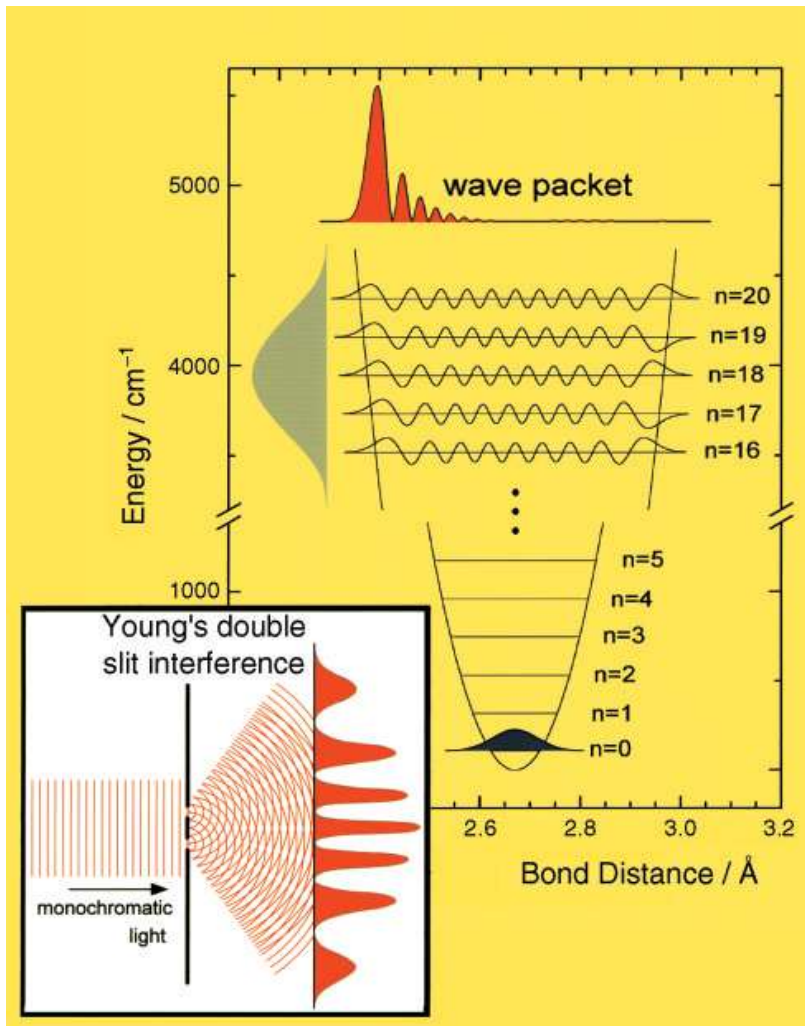
CSO 202 : Atoms Molecules and Photons



CSO 202 : Atoms Molecules and Photons

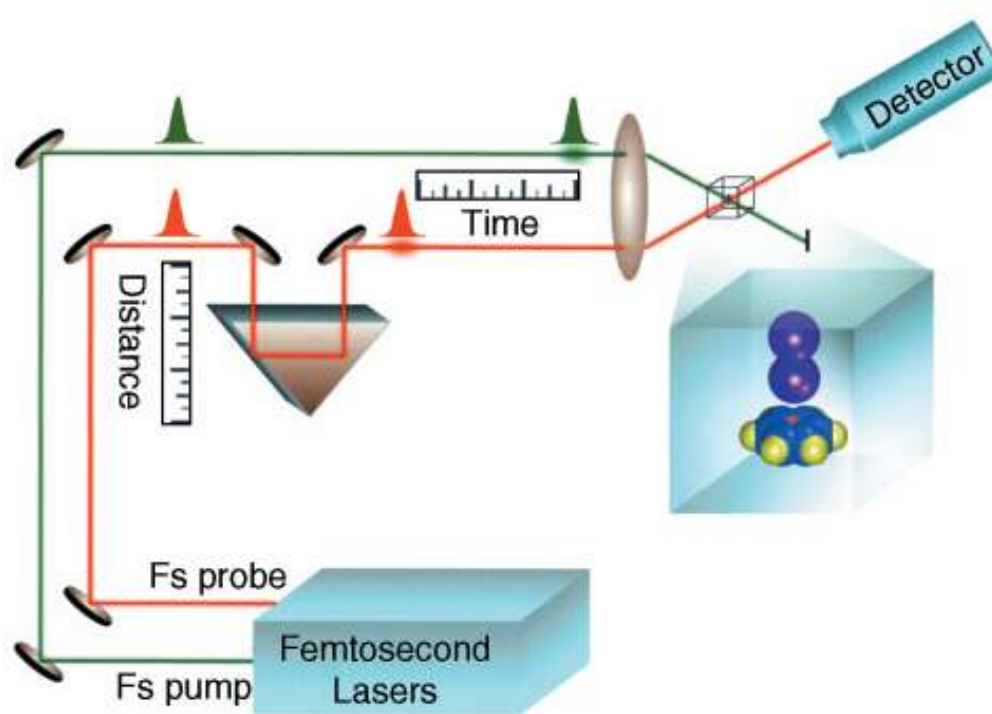






Diatomique molecule in un potentiel oscillateur harmonique: fonctions d'onde stationnaires et formation d'un paquet d'onde localisé. Paquet d'onde cohérent, localisé (de Broglie) calculé pour une molécule diatomique (iode) pour un pulsat de 20 fs. La différence avec la limite de fonction d'onde diffuse (nombre quantique n) est évidente.

Inset: Thomas Young's experiment (1801) on the interference of light.



The concept of femtosecond (pump-probe) experiments. After the probe pulse has been delayed by diversion through a variable length optical path, femtosecond pump and probe pulses are focused into a volume containing the molecules to be studied. The detector responds to the probe pulse by any of a variety of schemes

CSO 202 : Atoms Molecules and Photons

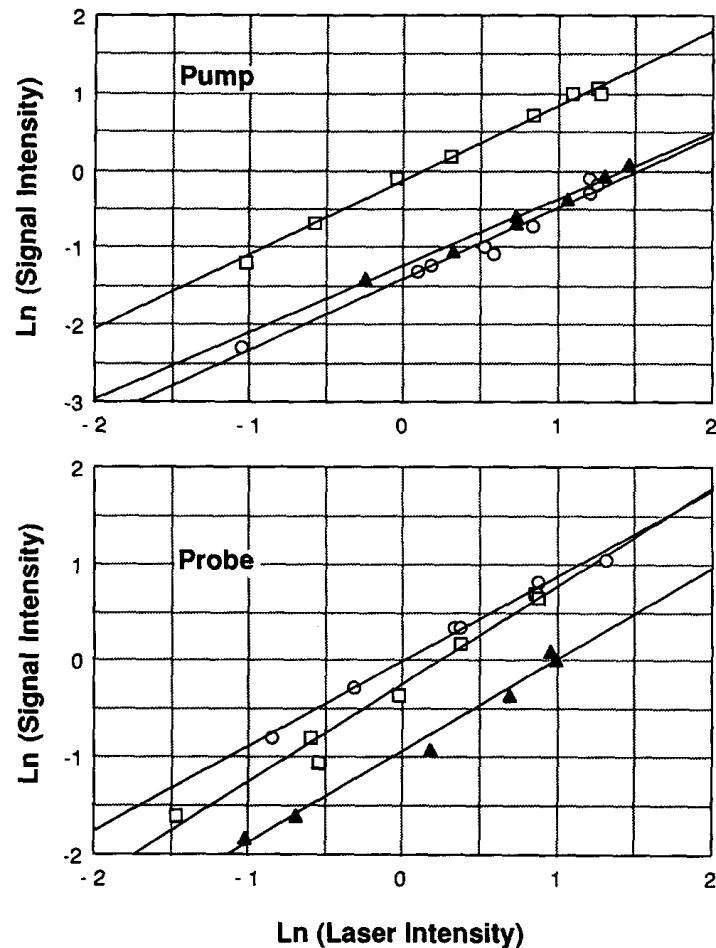


FIG. 3. Power dependence of the LIF signal. The observed LIF is plotted as a function of the pump or probe intensity on a log-log scale. Key: open squares: on-resonance transients; solid triangles and open circles: off-resonance transients for different time delays. The lines shown are best fits to the data. Note that, in all cases, the slopes of the lines are near unity.

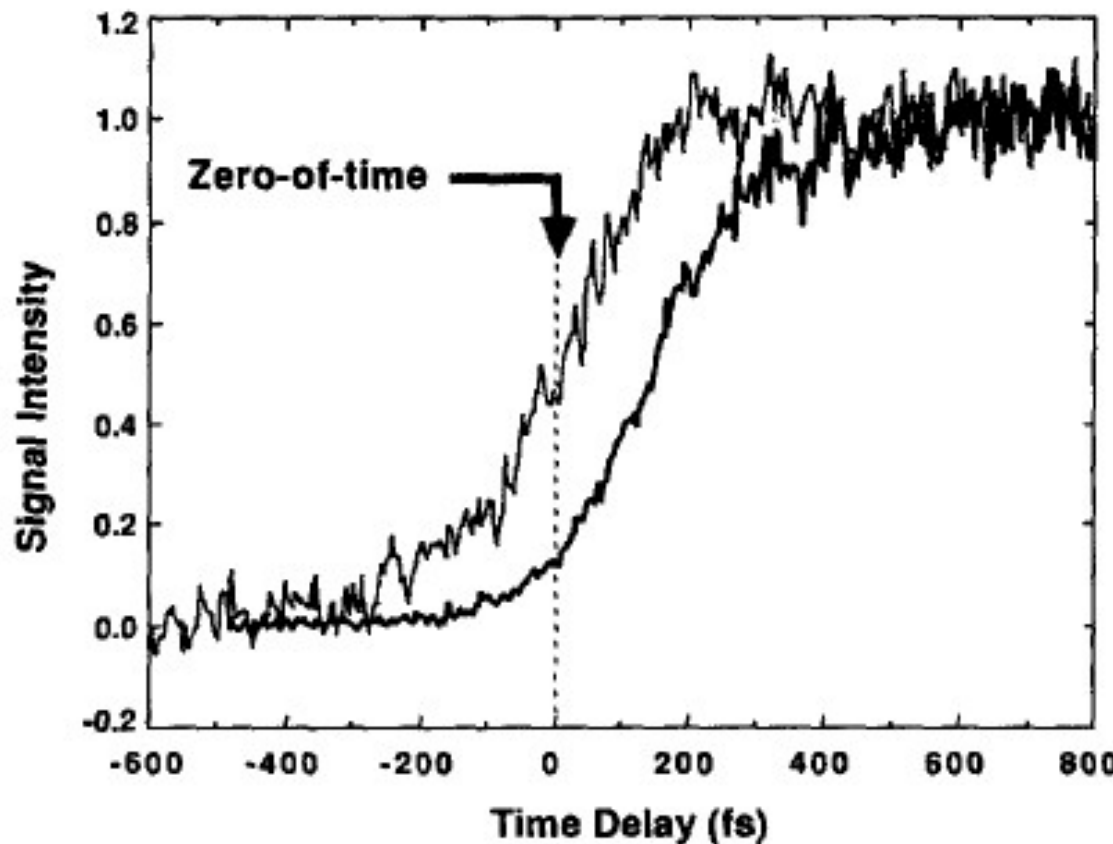
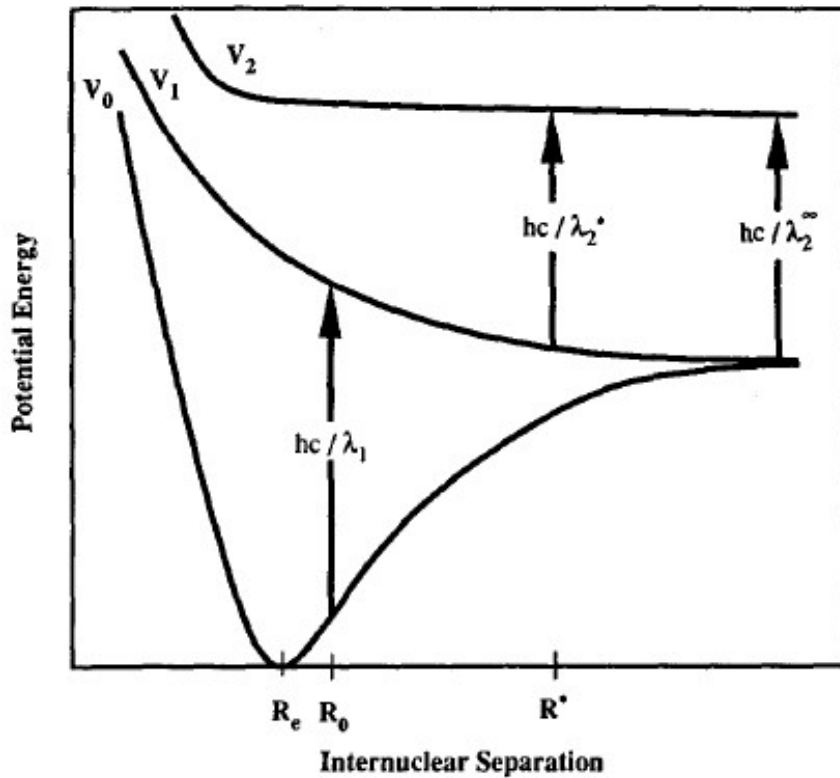


FIG. 6. Typical on-resonant FTS results for the ICN reaction. Top: The thin line is the MPI signal of DEA, which gives the detection-response function and the zero-of-time, as indicated (see text and paper II). The darker line is the FTS data for ICN, taken with $\lambda_2 = \lambda_2^*$. Note the time delay between these traces, $\tau_{1/2}$.



The PES's of an idealized molecule. V_0 , is the PES of the ground state, which has its minimum at $R = R_e$. At time $t = 0$, a pump photon of wavelength λ_1 is absorbed, as indicated by the vertical transition to V_1 . The internuclear separation increases as the system evolves on this repulsive potential. At time $t = \tau$, a pulse of wavelength λ^* (or λ^∞) probes the vertical transition from V_1 to a higher PES, V_2 .

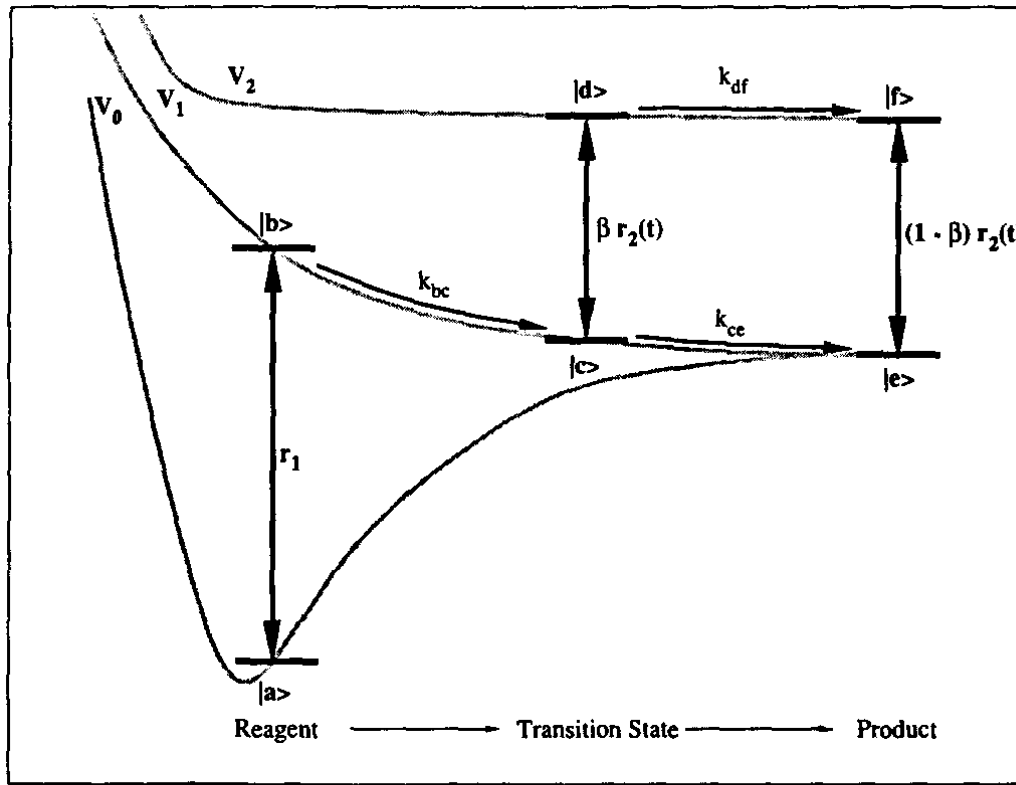


FIG. 9. Schematic of the simple kinetic (six-level) model. The continuum of transition states is described as a single pair ($|c\rangle$, $|d\rangle$) of states. The pumping and probing rates are $r_1(t)$ and $r_2(t)$, respectively. The k_{ij} give the spontaneous transition rates from $|i\rangle$ to $|j\rangle$, as shown. β is defined in the text. Stimulated emission by the pump and probe is indicated by the double headed arrows.

We get the following coupled rate equation

$$\begin{bmatrix} \dot{n}_a \\ \dot{n}_b \\ \dot{n}_c \\ \dot{n}_d \\ \dot{n}_e \\ \dot{n}_f \end{bmatrix} = \begin{bmatrix} -r_1(t) & r_1(t) & 0 & 0 & 0 & 0 \\ r_1(t) & -k_{bc} - r_1(t) & 0 & 0 & 0 & 0 \\ 0 & k_{bc} & -k_{ce} - \beta r_2(t) & \beta r_2(t) & 0 & 0 \\ 0 & 0 & \beta r_2(t) & -k_{df} - \beta r_2(t) & 0 & 0 \\ 0 & 0 & k_{ce} & 0 & -(1-\beta)r_2(t) & (1-\beta)r_2(t) \\ 0 & 0 & 0 & k_{df} & (1-\beta)r_2(t) & -(1-\beta)r_2(t) \end{bmatrix} \begin{bmatrix} n_a \\ n_b \\ n_c \\ n_d \\ n_e \\ n_f \end{bmatrix}$$

where we make the following definitions:

$n_i(t)$ ≡ the instantaneous population of state $|i\rangle$,

k_{ij} ≡ the rate of spontaneous decay of molecules from state $|i\rangle$ to state $|j\rangle$,

$r_1(t)$ ≡ the instantaneous rate at which the pump pulse excites from state $|a\rangle$ to state $|b\rangle$,
and

$r_2(t)$ ≡ the instantaneous rate at which the probe pulse excites from state $|c\rangle$ to state $|d\rangle$ and from $|e\rangle$ to $|f\rangle$

Further, β is defined as a dimensionless parameter describing the relative ratio of the two probe absorptions.

Thus, by definition, $\beta = 1$ if the probe is tuned perfectly to the transition-state absorption ($|c\rangle \rightarrow |d\rangle$), whereas $\beta = 0$ if the probe is tuned completely to the final state transition ($|e\rangle \rightarrow |f\rangle$). The rate at which the pump excites the system (from $|a\rangle$ to $|b\rangle$) is given by

$$r_1(t) = I_1(t)\sigma_{ab}\lambda_1/hc,$$

and, similarly for the probe,

$$r_2(t) = I_2(t)\sigma_{ef}\lambda_2/hc.$$

Boundary conditions

$$n_a(-\infty) = N,$$

$$n_b(-\infty) = \dots = n_f(-\infty) = 0,$$

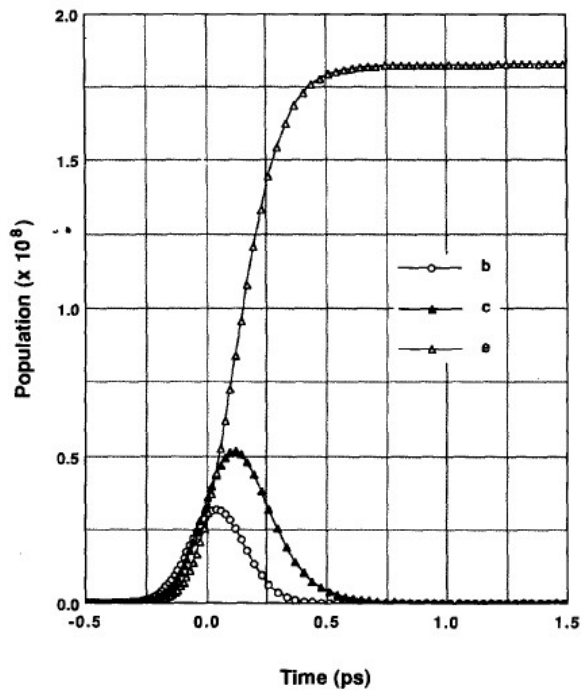


FIG. 10. Population evolution of the simple kinetic model. The instantaneous population of three of the six states are shown as a function of time. Key: open circles = $n_b(t)$, solid triangles = $n_c(t)$, open triangles = $n_e(t)$. Assumed parameters (see the text for definitions): $k_{ba} = 2 \times 10^{13} \text{ s}^{-1}$, $k_{ce} = k_{df} = 10^{13} \text{ s}^{-1}$, τ (delay time) = 500 fs, $N = 10^{12}$ molecules, $\sigma_{ab} = 4 \times 10^{-20} \text{ cm}^2$, $\sigma_{cd} = 5 \times 10^{-17} \text{ cm}^2$, and $\beta = 0.95$. In addition, the energies of the pump and probe beams were taken to be 150 and 50 nJ, respectively, with a common width of 150 fs and beam radius of 40 μm . Note that for ~ 250 fs, the population of the transition state (n_c) is a significant fraction of that of the final state (n_e).

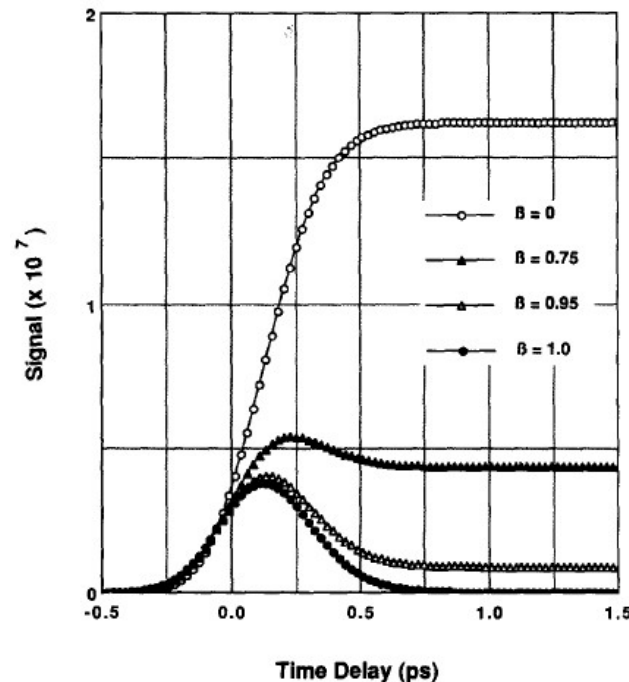


FIG. 11. Predicted FTS results from the simple kinetic model. The signal was calculated using the same parameters as for Fig. 10, as a function of the tuning parameter β . Key: open circles: $\beta = 0$; solid triangles: $\beta = 0.75$; open triangles: $\beta = 0.95$; and solid circles: $\beta = 1.0$. Here, the signal is the population in level $|f\rangle$ (sampled at long times; see Fig. 10) as a function of pump-probe delay time.

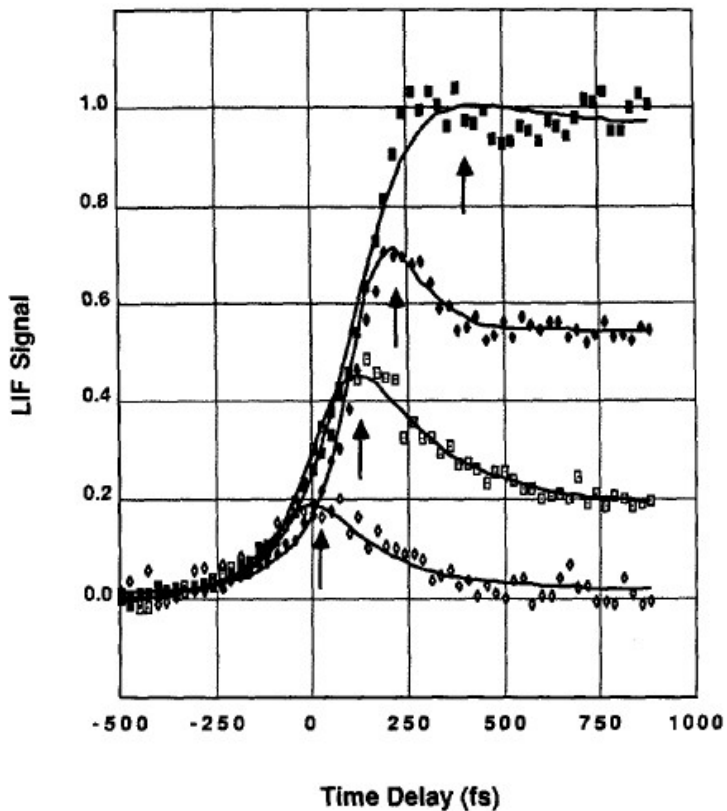
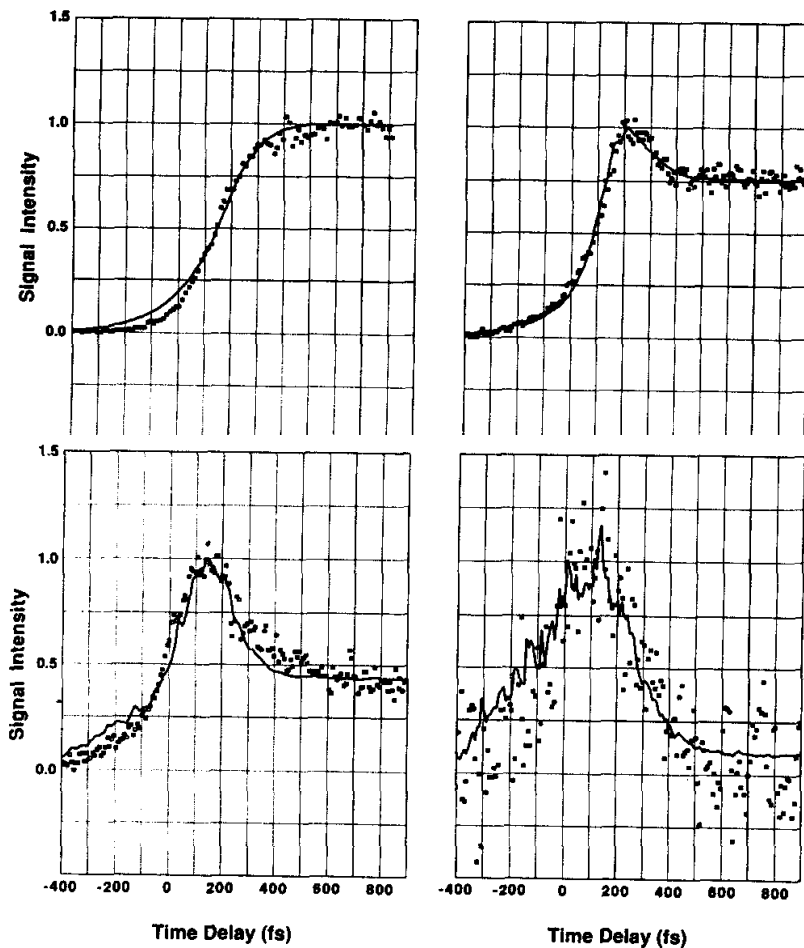
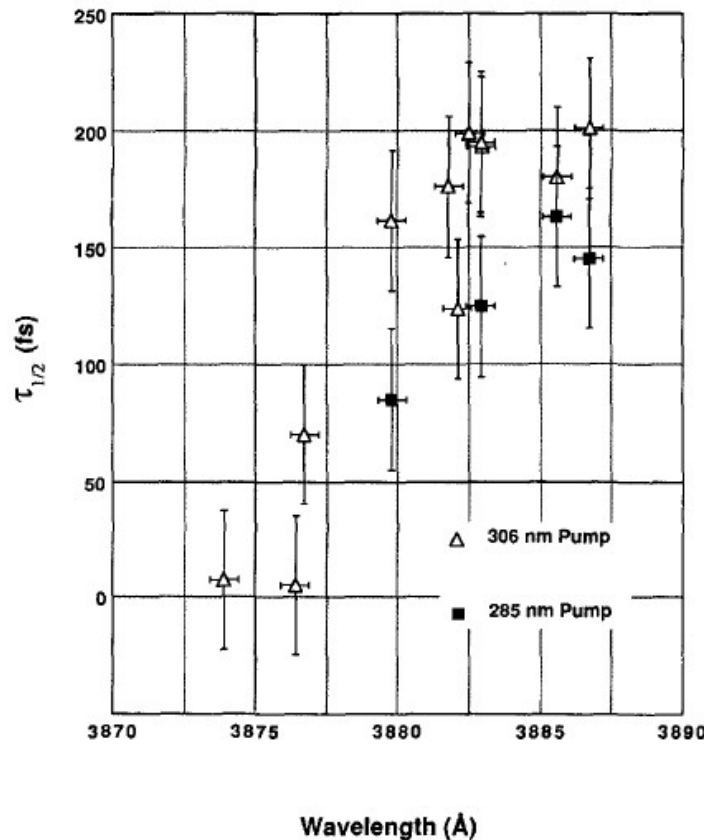


FIG. 7. Typical off-resonant FTS results for the ICN reaction. Key: solid squares: $\lambda_2 = 389.7$ nm; solid diamonds: $\lambda_2 = 389.8$ nm; open squares $\lambda_2 = 390.4$ nm; open diamonds: $\lambda_2 = 391.4$ nm. The zero-of-time is determined separately for each data set using the DEA-MPI technique. The solid lines and arrows are guides to the eye, showing the approximate peak positions for each data set.



Tuning to the Red

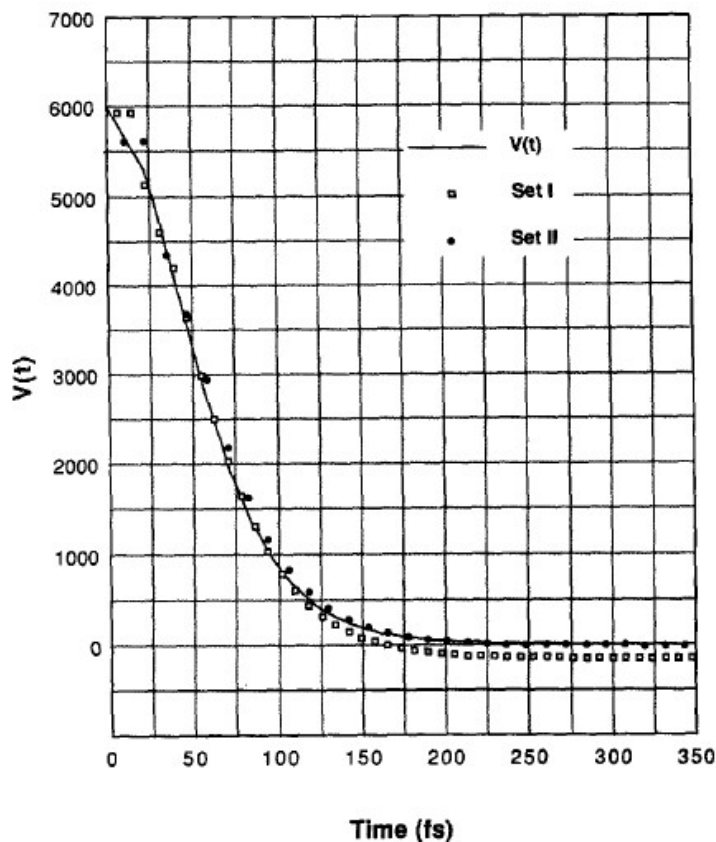
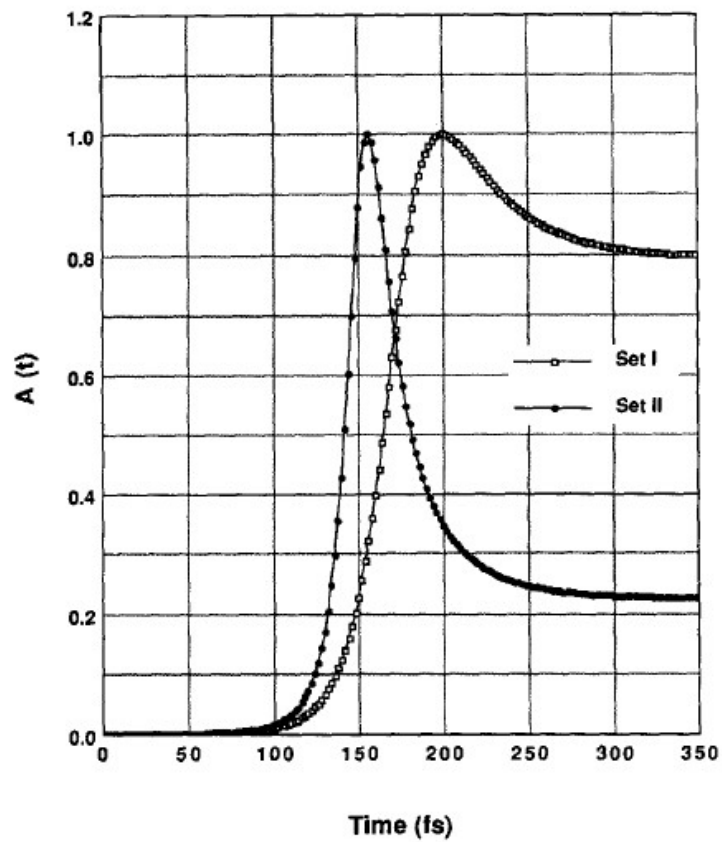
FIG. 5. Typical ICN transients as a function of probe wavelength. The probe wavelengths were (a) $\lambda_2^* = 388.9$ nm, (b) $\lambda_2^* = 389.8$ nm, (c) $\lambda_2^* = 390.4$ nm, and (d) $\lambda_2^* = 391.4$ nm. The solid lines were generated by fitting the classical model of Eq. (5) convolved with the measured experimental response for each transient.



Tuning to the Blue

FIG. 8. Delay time as a function of probe wavelength. The values of $\tau_{1/2}$ obtained are shown for an approximate pump wavelength of 306 nm (open triangles) and 285 nm (solid squares). The FWHM of the probe was $\sim 60 \text{ cm}^{-1}$ in each case.

CSO 202 : Atoms Molecules and Photons



CSO 202 : Atoms Molecules and Photons

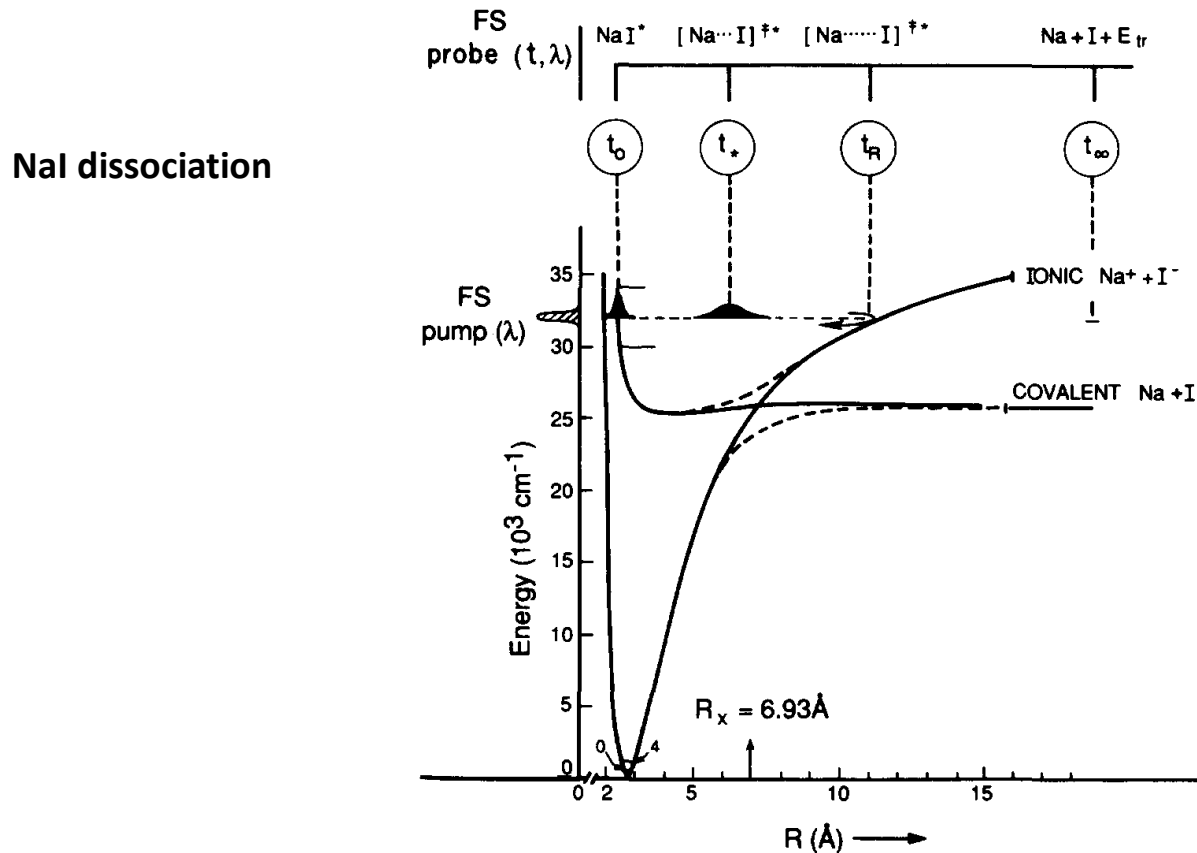


FIG. 1. A display of the potential energy surfaces involved, and the method of FTS. The times t_0 , t_* , t_R , and t_∞ refer to the time of evolution of packet as it moves along the coordinate R and spreads. At the top of the figure, the different transition configurations are given. The fs pump pulse was at 310 nm, and the probe was generated from a continuum ($\lambda = 560$ nm to $\lambda = 630$ nm). The $\text{Na} + \text{I}$ product states correlate with the states ($\Omega = 0^+$ and 1) of NaI and are depicted by the covalent surface in this figure. In our full report later we will discuss details of the dynamics on these surfaces.

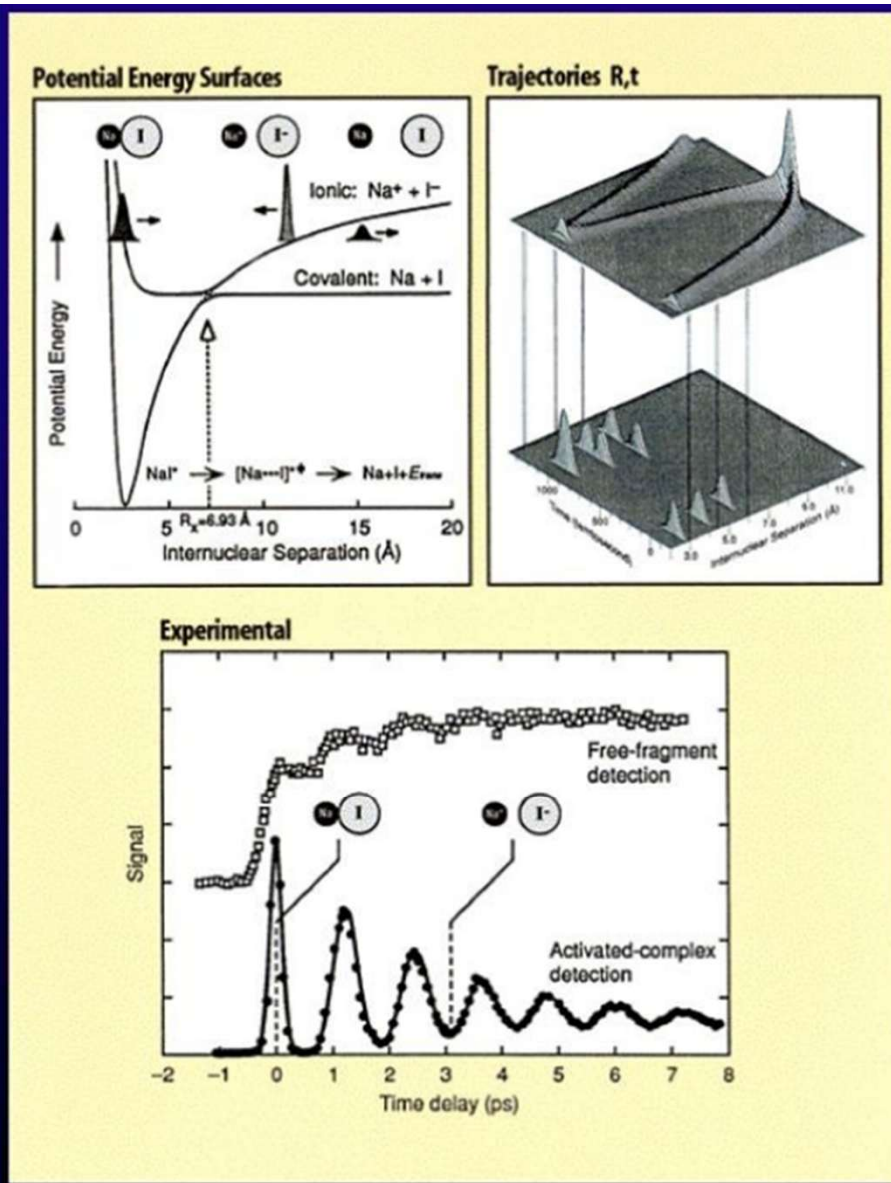


Figure 7

Femtochemistry of the NaI reaction, the paradigm case. The experimental results show the resonance motion between the covalent and ionic structures of the bond, and the time scales for the reaction and for the spreading of the wave packet. Two transients are shown for the activated complexes in transition states and for final fragments. Note the "quantized" behavior of the signal, not simply an exponential rise or decay of the ensemble. The classical motion is simulated as trajectories in space and time.

CSO 202 : Atoms Molecules and Photons

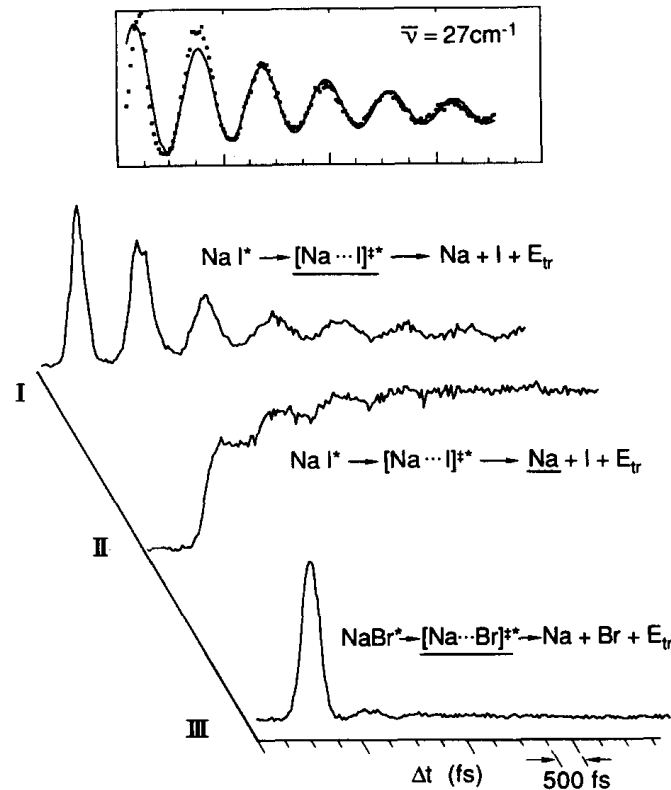
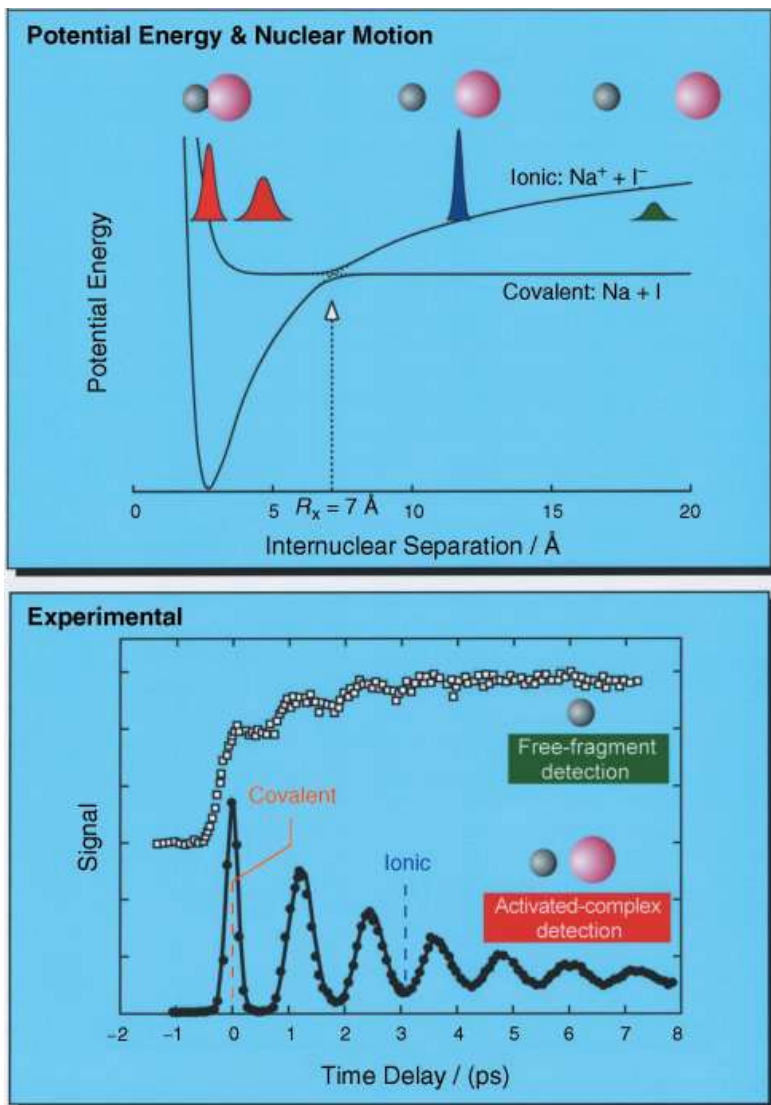


FIG. 2. Experimental results for the two reactions of NaI and NaBr. For the NaI reaction, we provide both the on-resonance and off-resonance Na atom detection (LIF), indicated by the underlining of the relevant species. Results, not shown, were also obtained at a number of other wavelengths, and will be detailed later. The modulation depth depends on the probe wavelength. The two salts (Aldrich, purity 99.9%) were degassed under vacuum for over 8 h (400 °C), and heated to ~600 °C. The experiments were also repeated at lower temperatures to check for dimerization. The signal is (essentially) linearly dependent on the probe and pump intensities.

CSO 202 : Atoms Molecules and Photons



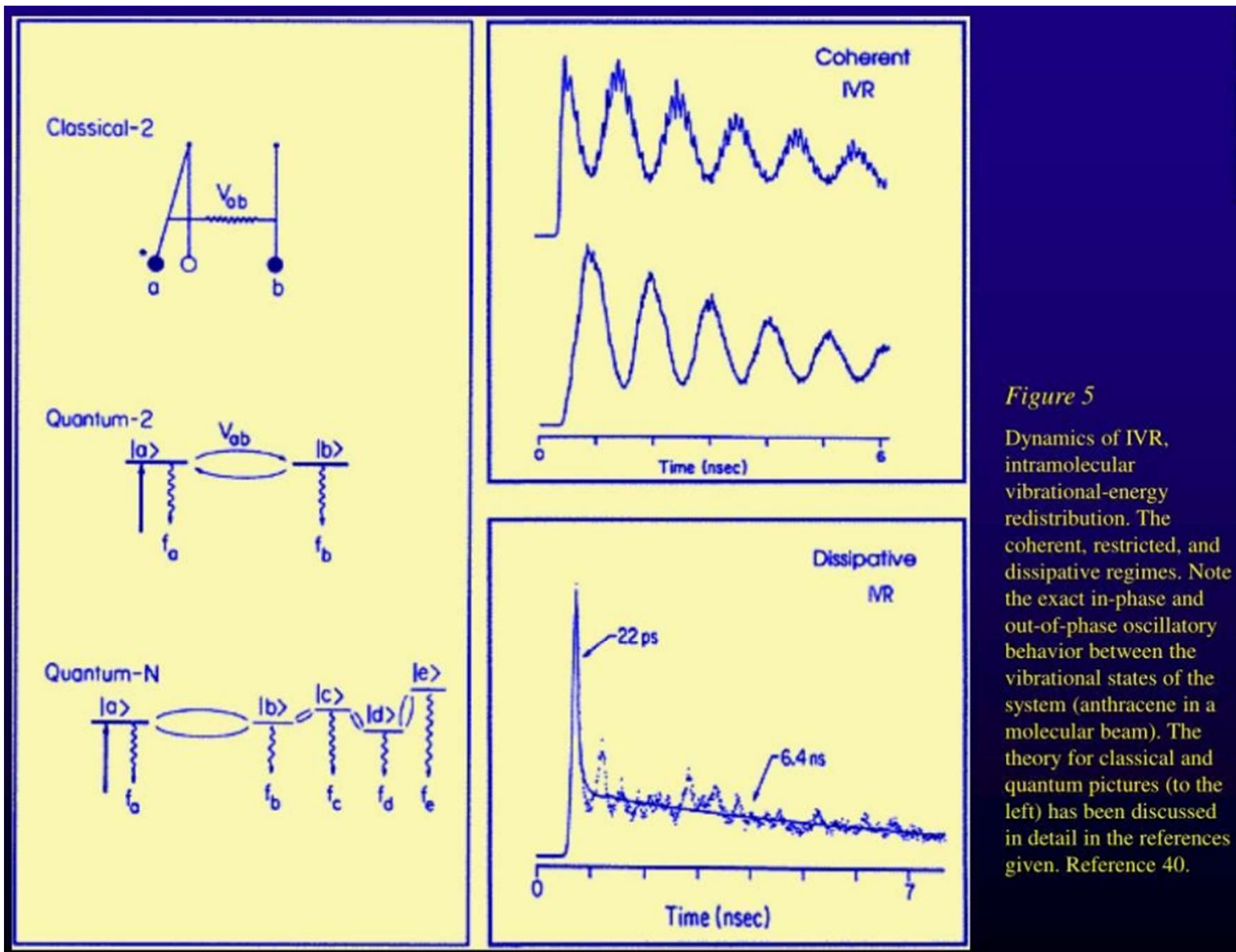


Figure 5

Dynamics of IVR, intramolecular vibrational-energy redistribution. The coherent, restricted, and dissipative regimes. Note the exact in-phase and out-of-phase oscillatory behavior between the vibrational states of the system (anthracene in a molecular beam). The theory for classical and quantum pictures (to the left) has been discussed in detail in the references given. Reference 40.

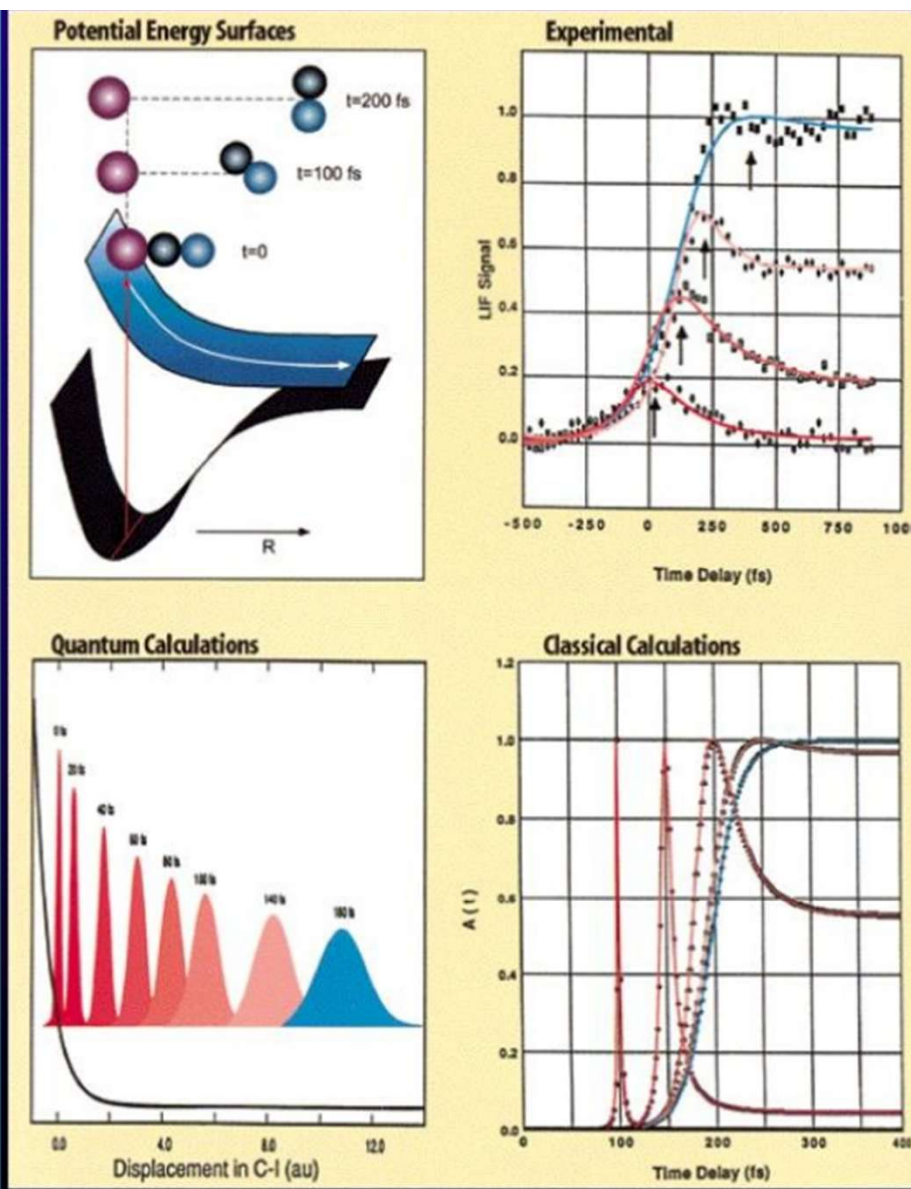


Figure 6

Femtochemistry of the ICN reaction, the first to be studied. The experimental results show the probing of the reaction in the transition-state region (rise and decay) and the final CN fragment (rise and leveling) with precise clocking of the process; the total time is 200 fs. The I fragment was also detected to elucidate the translational energy change with time. Classical and quantum calculations are shown.

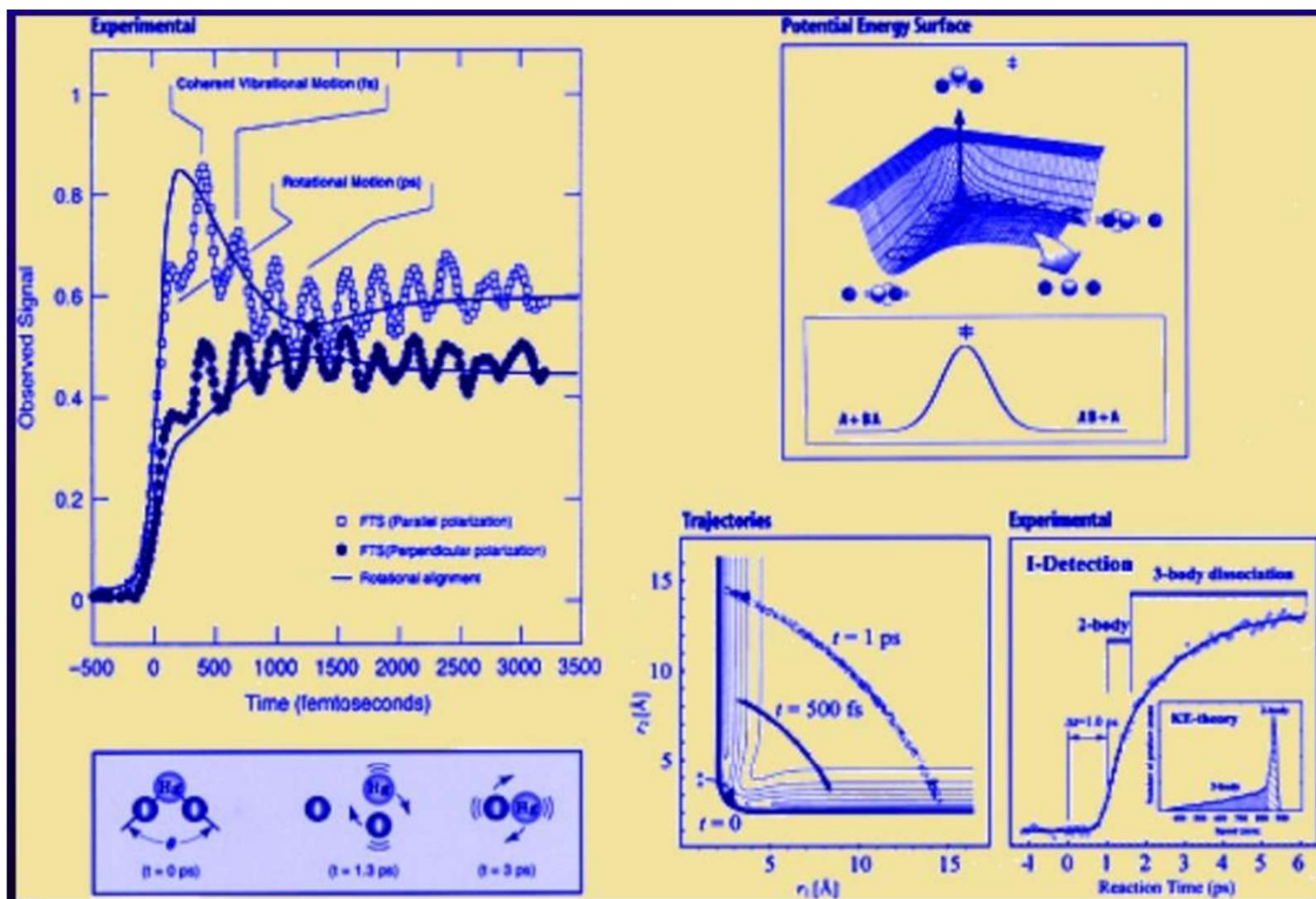


Figure 8 Femtochemistry of the IHgI reaction, the saddle-point transition state (barrier reactions). The experimental results show both the coherent vibrational and rotational motions of the reaction (left). The transition state IHgI^* and final fragment HgI were probed. We also probed the I fragment and the change of translational energy with time. The classical trajectory calculations are shown (right), together with experimental results for I detection; both theory and experiment illustrate the family of reaction trajectories on the global PES, in time and in kinetic energy distribution. Quantum calculations were also made (not shown). This ABA system is a prototype for saddle-point transition states. Reference 43.

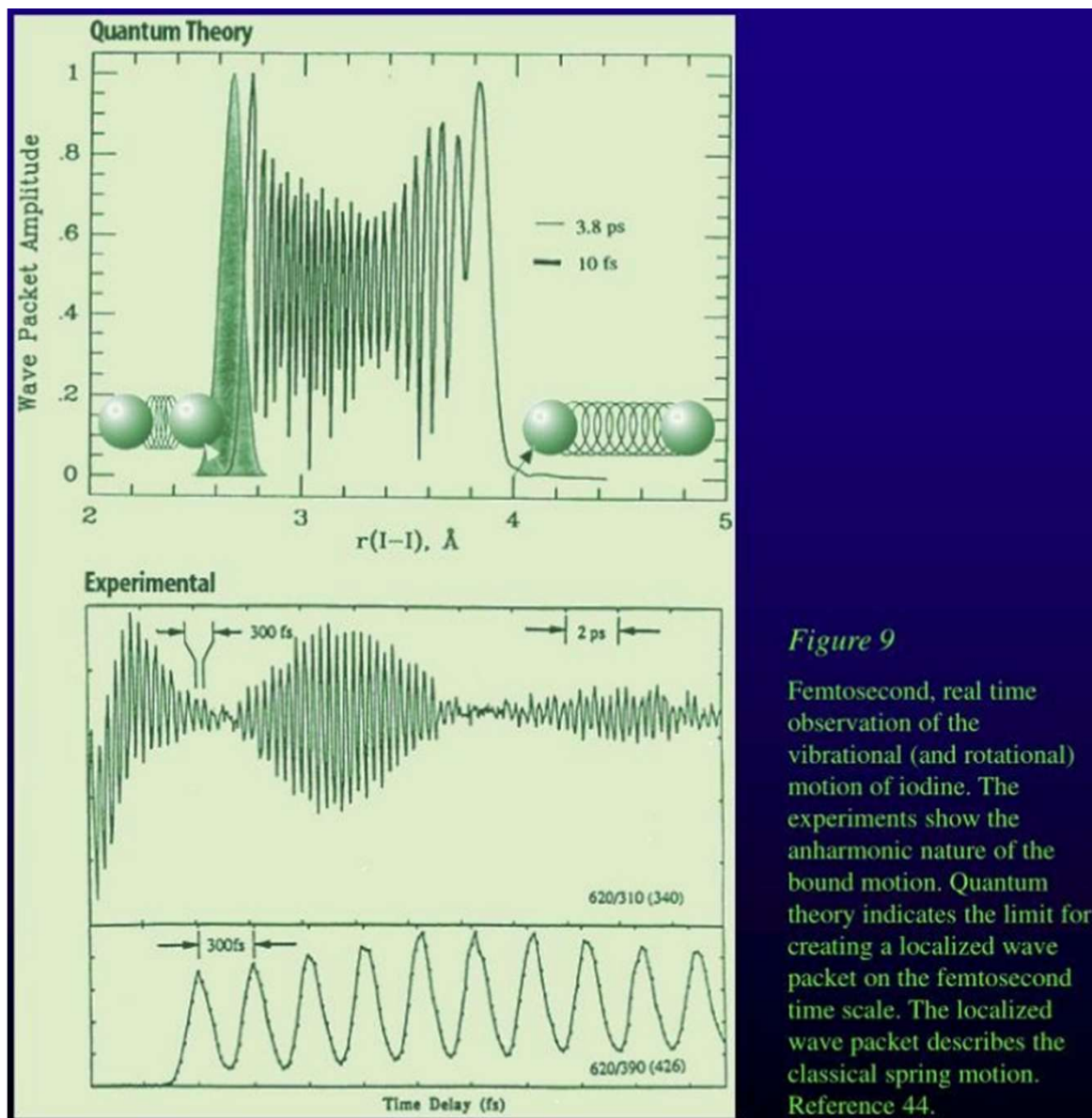
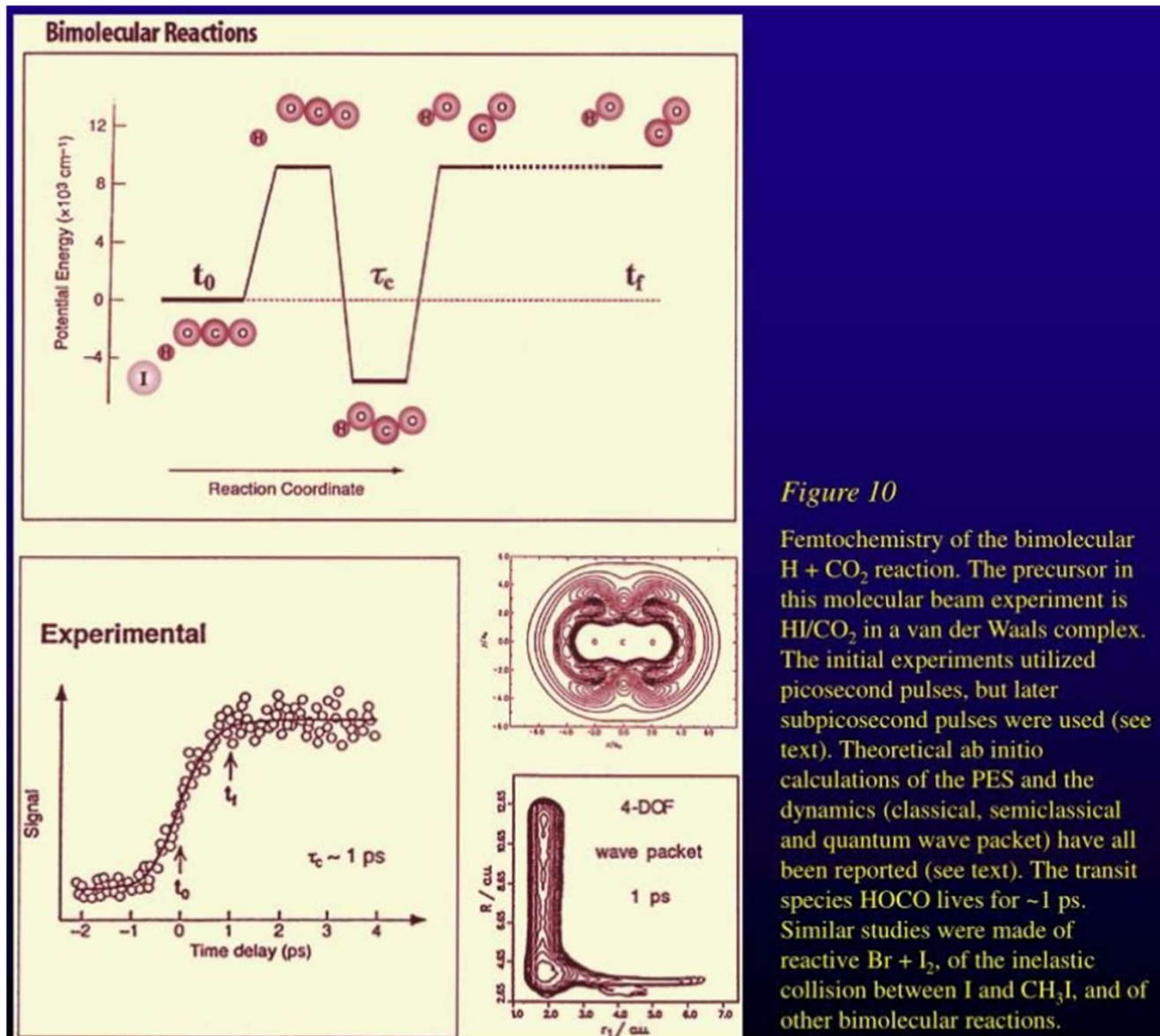


Figure 9

Femtosecond, real time observation of the vibrational (and rotational) motion of iodine. The experiments show the anharmonic nature of the bound motion. Quantum theory indicates the limit for creating a localized wave packet on the femtosecond time scale. The localized wave packet describes the classical spring motion. Reference 44.



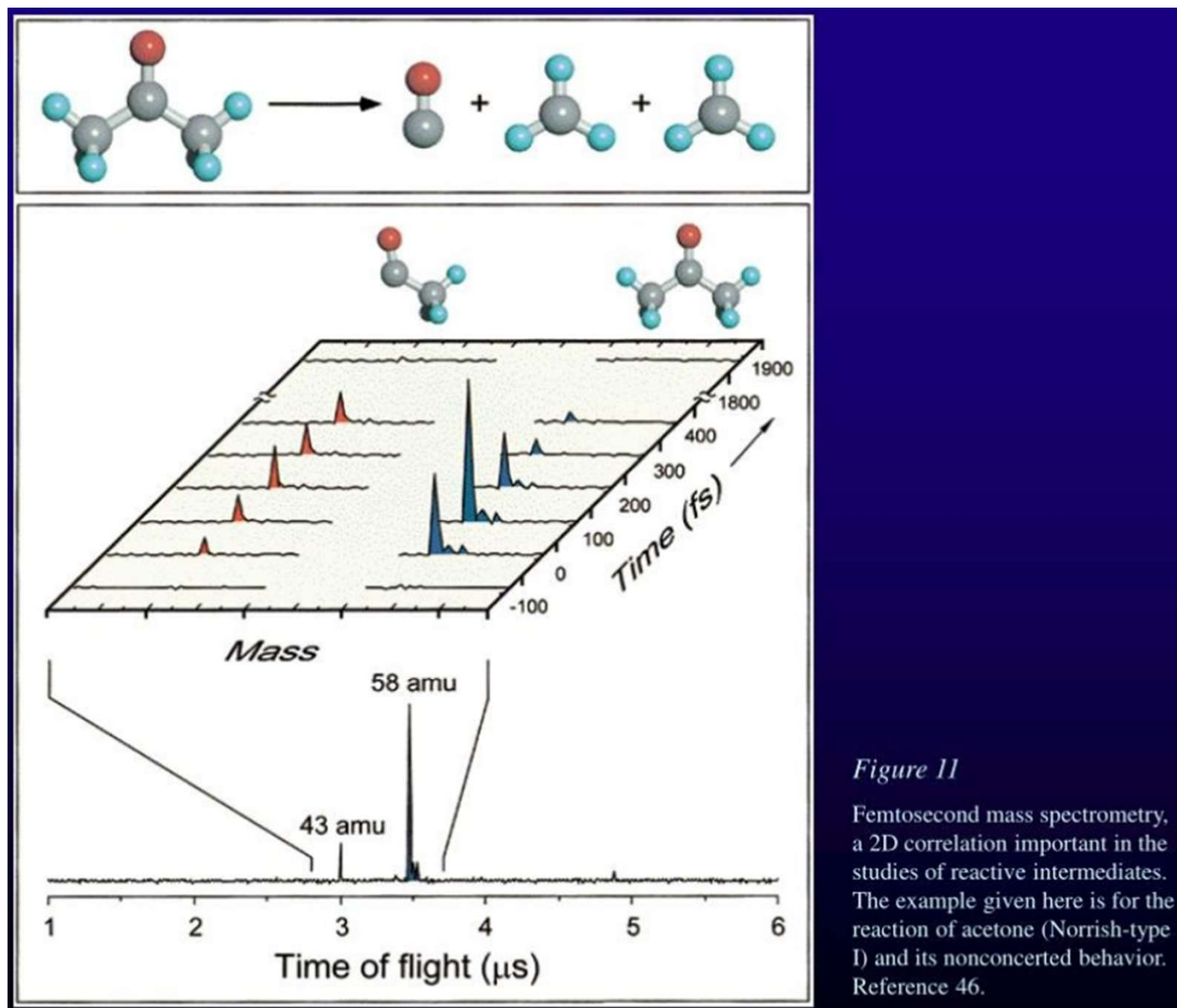


Figure II

Femtosecond mass spectrometry, a 2D correlation important in the studies of reactive intermediates. The example given here is for the reaction of acetone (Norrish-type I) and its nonconcerted behavior. Reference 46.

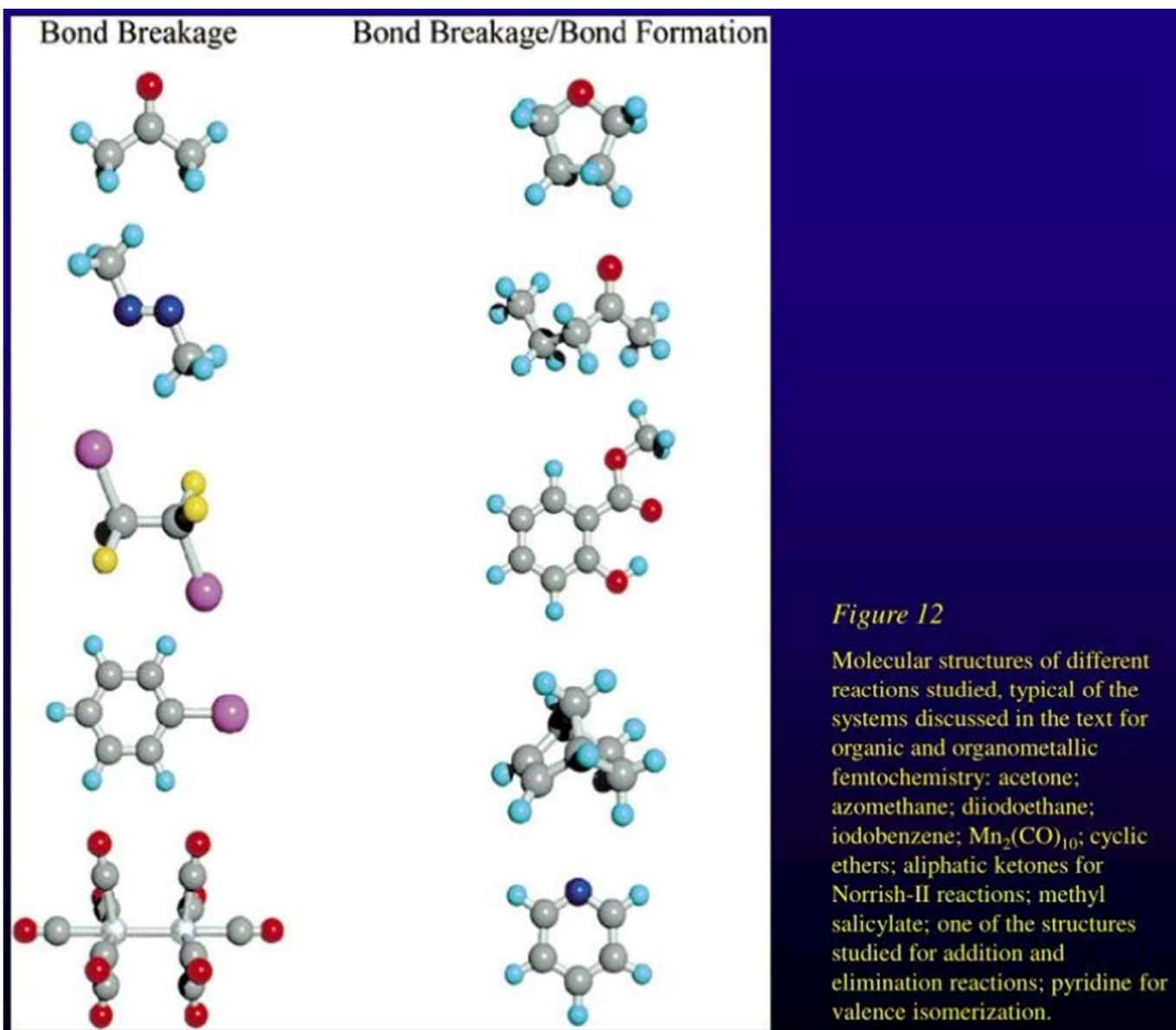


Figure 12

Molecular structures of different reactions studied, typical of the systems discussed in the text for organic and organometallic femtochemistry: acetone; azomethane; diiodoethane; iodobenzene; $\text{Mn}_2(\text{CO})_{10}$; cyclic ethers; aliphatic ketones for Norrish-II reactions; methyl salicylate; one of the structures studied for addition and elimination reactions; pyridine for valence isomerization.

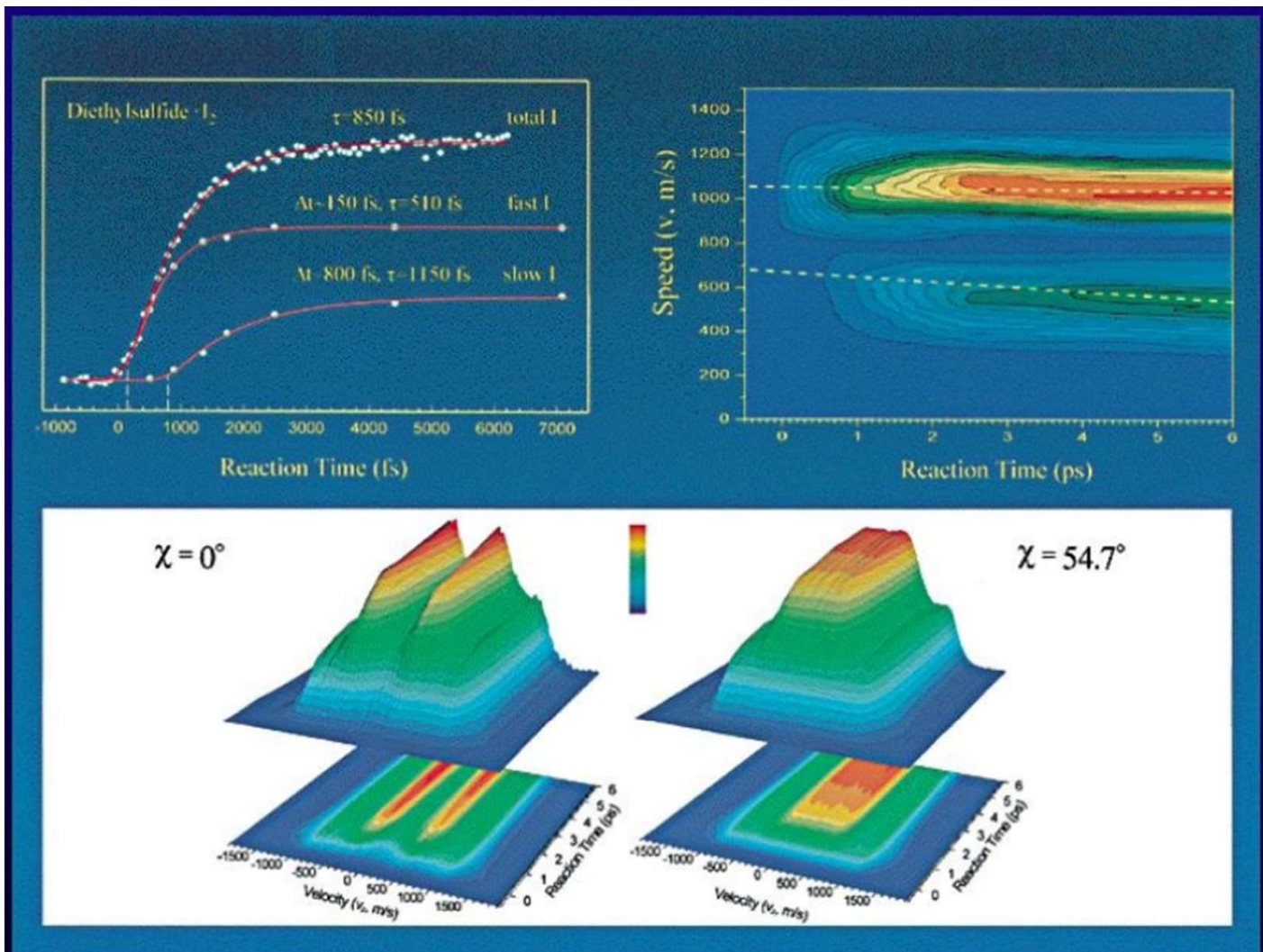


Figure 13 Femtochemistry of bimolecular electron-transfer reactions, the classic case of donors (e.g., benzene or diethyl sulfide) and acceptors (e.g., iodine or iodomonochloride). The experimental results clearly show the distinct velocity and time correlations, and thus the two-speed distributions and time scales of the reaction on the global PES. Reference 47.

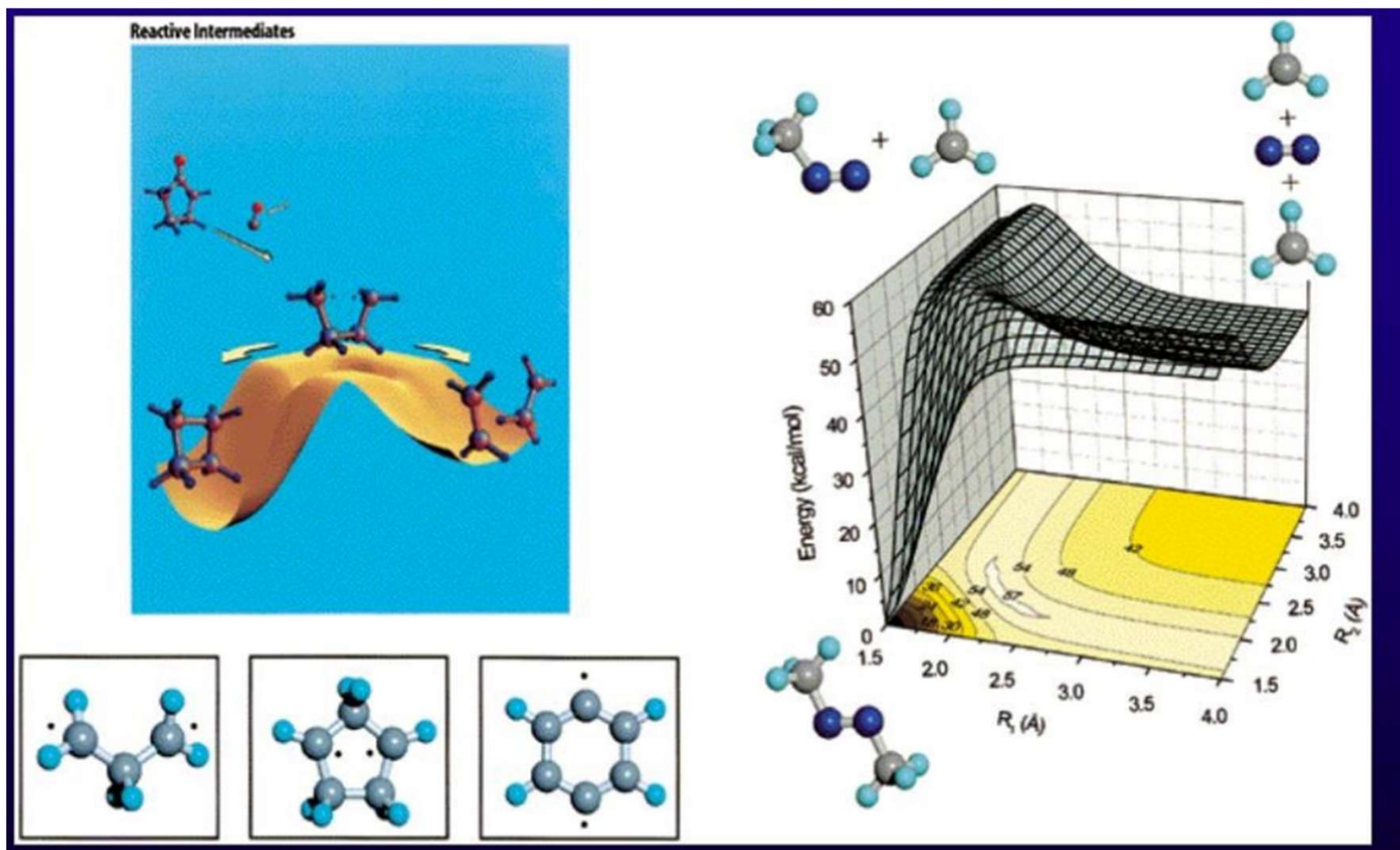
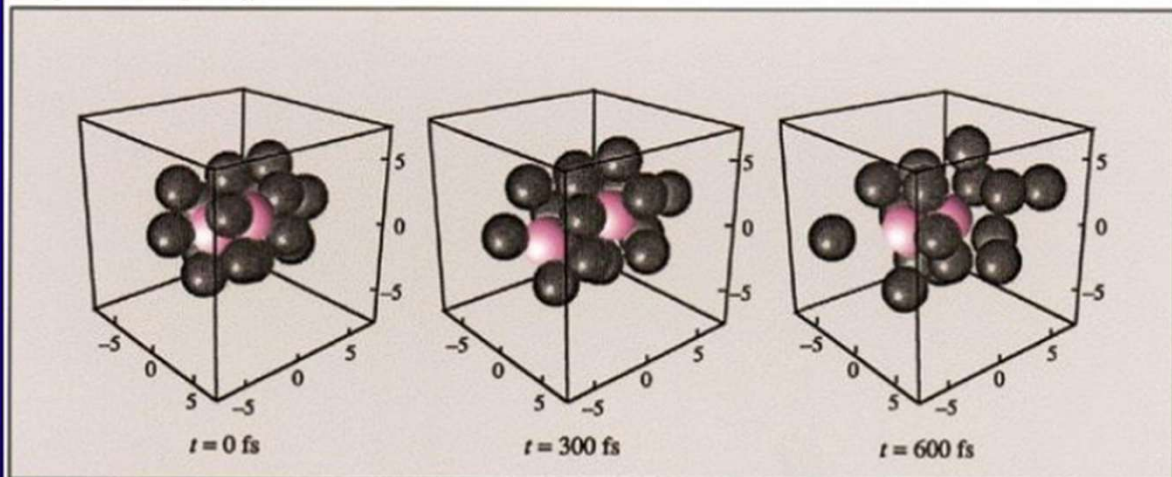


Figure 14 Reactive intermediates on the femtosecond time scale. (Left) Here, tetramethylene, trimethylene, bridged tetramethylene and benzyne are examples of species isolated on this time scale (see Figure 12 for others). (Right) Reaction dynamics of azomethane, based on the experimental, femtosecond studies. The ab initio PES was obtained from state-of-the-art calculations (E. Diau, this laboratory) which show the two reaction coordinates (C-N) relevant to the dynamics. A third coordinate, which involves a twisting motion, was also studied. Note the concerted and nonconcerted pathways. Reference 48.



Snapshots of $I_2 \cdot Ar_{17}$



Snapshots of $I_2 \cdot benzene_5$

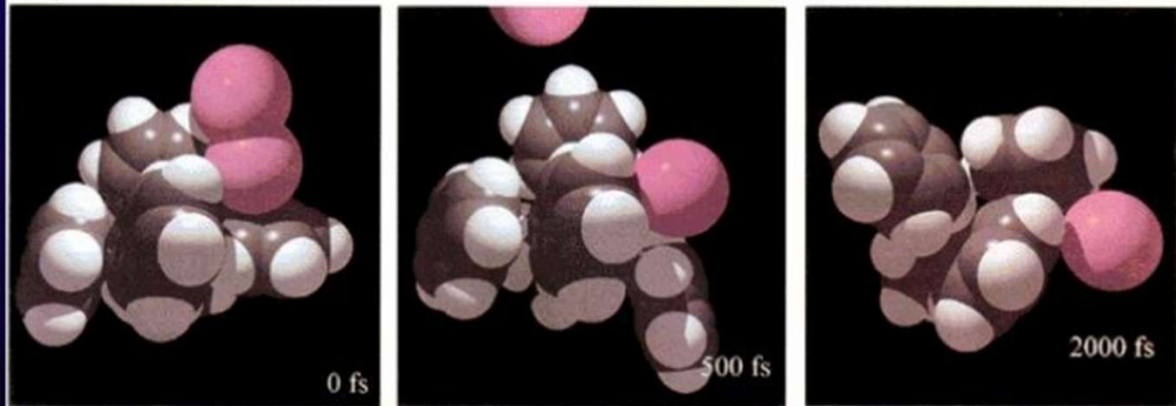


Figure 15 Femtosecond dynamics in the mesoscopic phase, reactions in solvent clusters. Two examples are given: The coherent nuclear dynamics of bond breakage and recombination of iodine in argon (the cage effect), and the dynamics of the same solute but in polyatomic solvents (benzene). It was for the former that the first coherent bond breakage in the cage was observed and separated from the effect of vibrational relaxation. For the latter, the two atoms experience different force fields and the time scales are determined by the degree of solvation. (We also studied van der Waals complexes.) Studies of acid-base reactions of naphthol with ammonia, changing the number of solvent molecules from 0 to 10, and the isomerization of stilbene (hexane as a solvent) were similarly made. Reference 49.

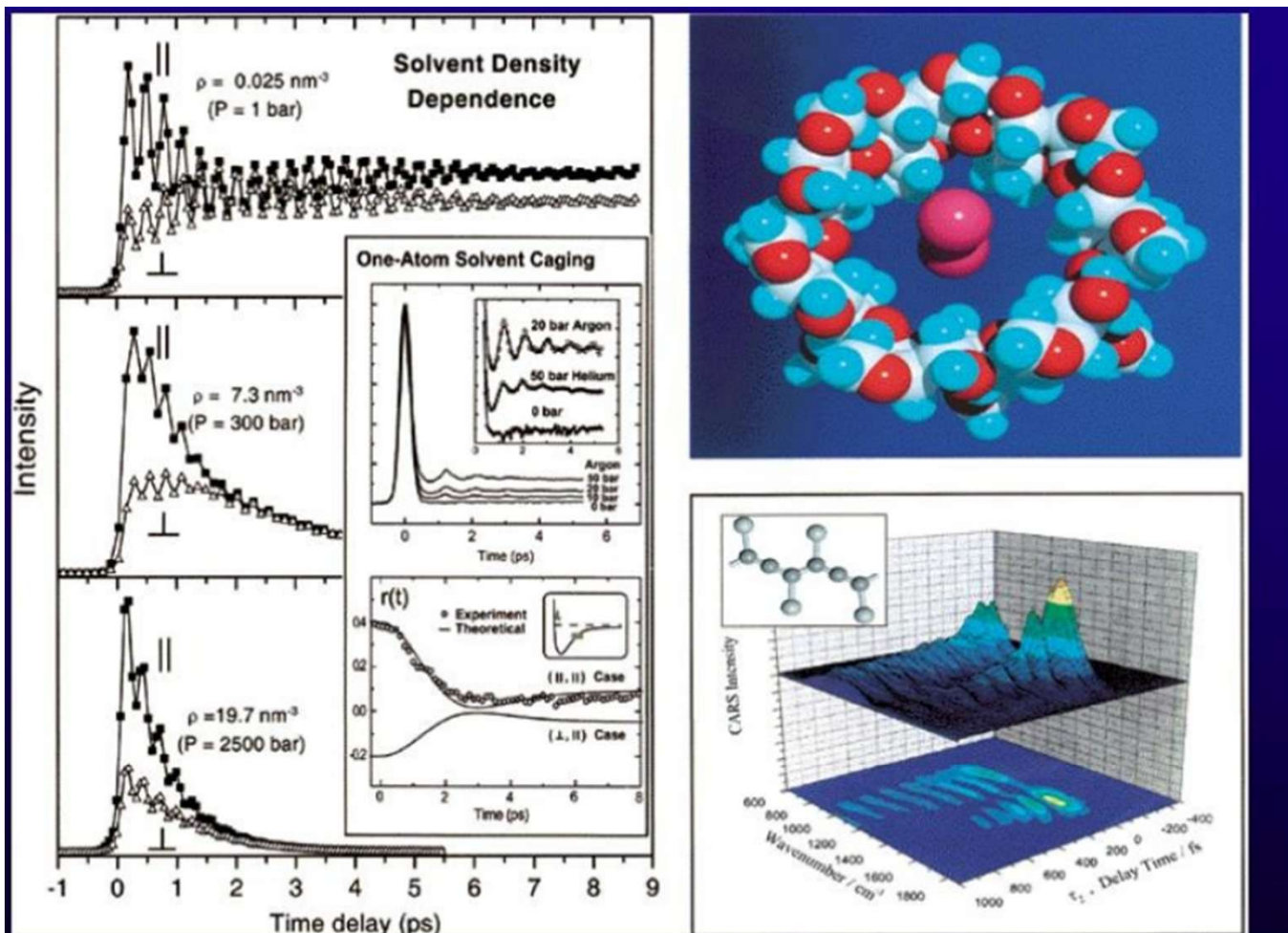


Figure 16 Femtosecond dynamics in the condensed phase: (left) coherent vibrational and rotational motions observed in dense fluids as a function of density and down to the one-atom collision with iodine; (right) nanocavities of cyclodextrins and polymers of polydiacetylenes; liquids (not shown, but references are given). Studies in these media include the one-atom coherent caging, J-coherence friction model, coherent IVR in polymer chains, and anomalous T2 behavior in dense fluids. Reference 50.

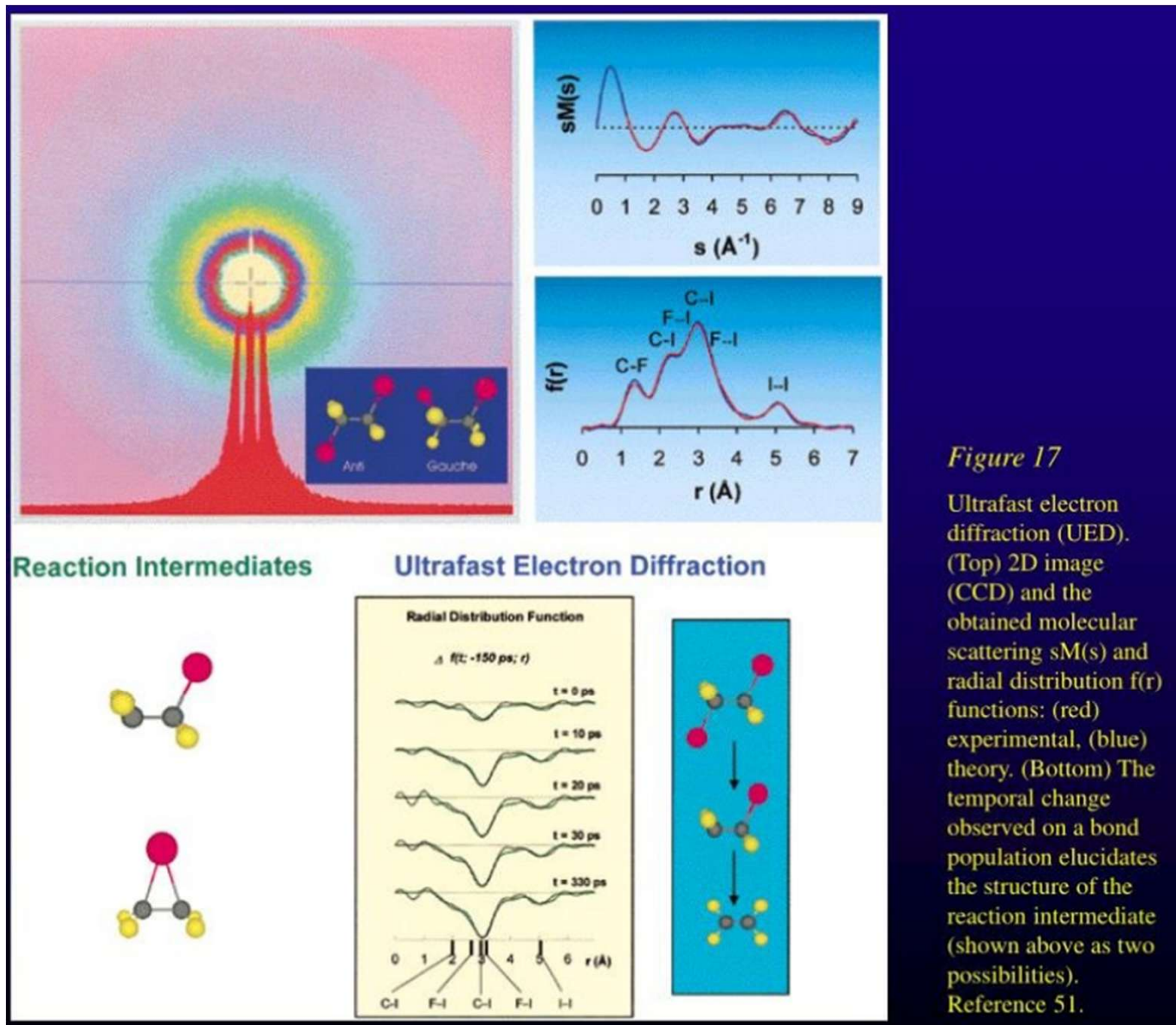


Figure 17

Ultrafast electron diffraction (UED). (Top) 2D image (CCD) and the obtained molecular scattering $sM(s)$ and radial distribution $f(r)$ functions: (red) experimental, (blue) theory. (Bottom) The temporal change observed on a bond population elucidates the structure of the reaction intermediate (shown above as two possibilities). Reference 51.

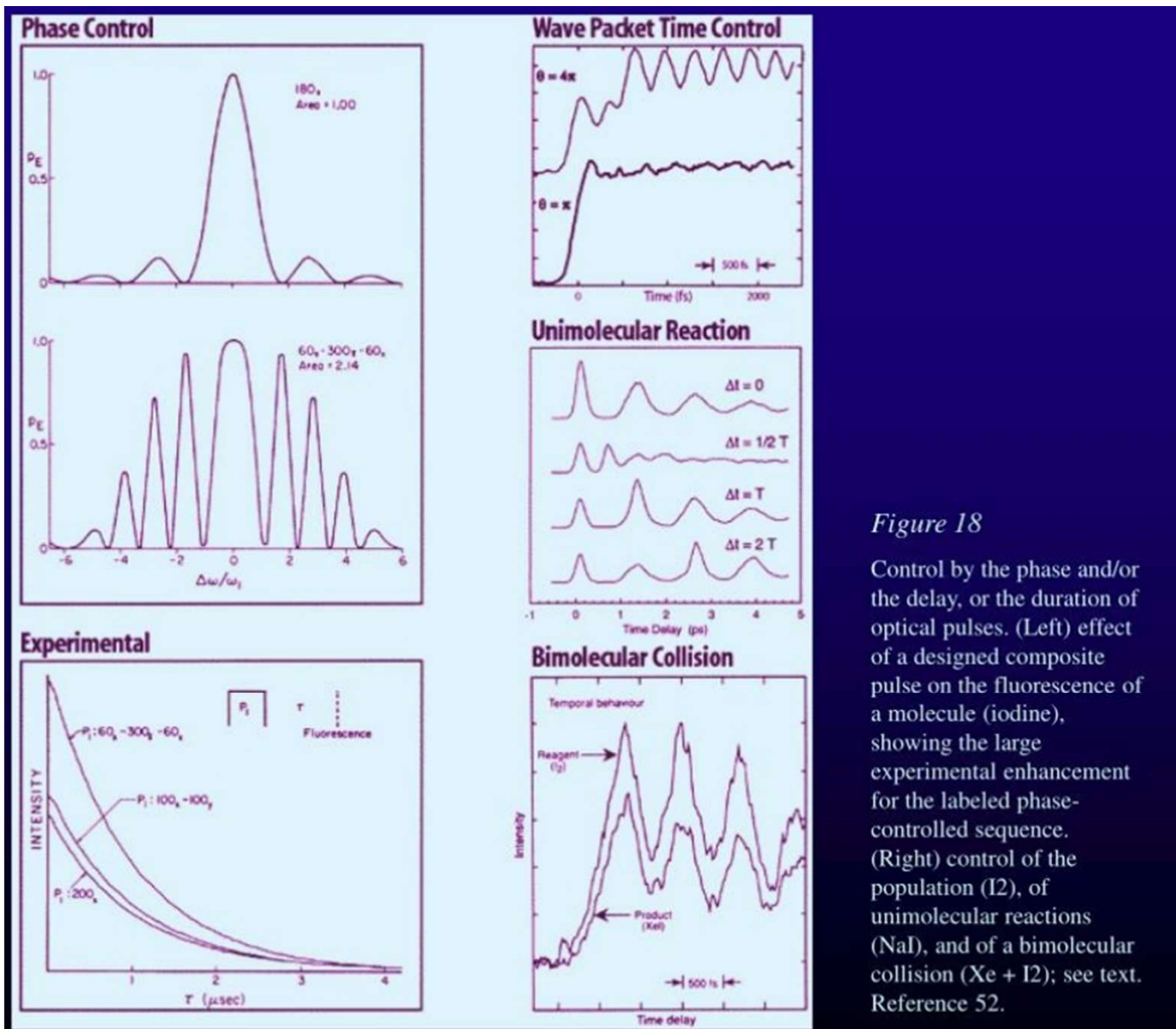


Figure 18

Control by the phase and/or the delay, or the duration of optical pulses. (Left) effect of a designed composite pulse on the fluorescence of a molecule (iodine), showing the large experimental enhancement for the labeled phase-controlled sequence. (Right) control of the population (I₂), of unimolecular reactions (NaI), and of a bimolecular collision (Xe + I₂); see text. Reference 52.

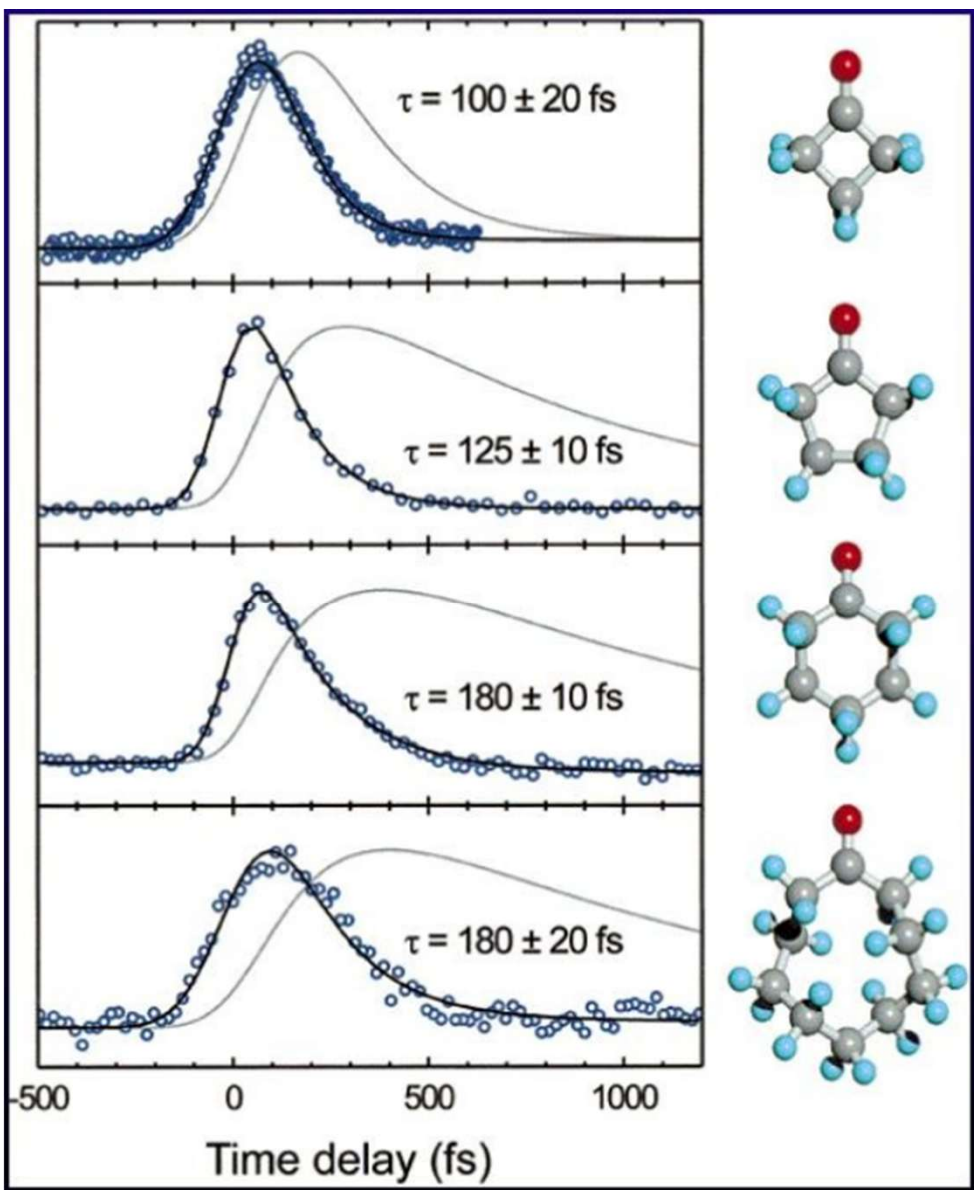
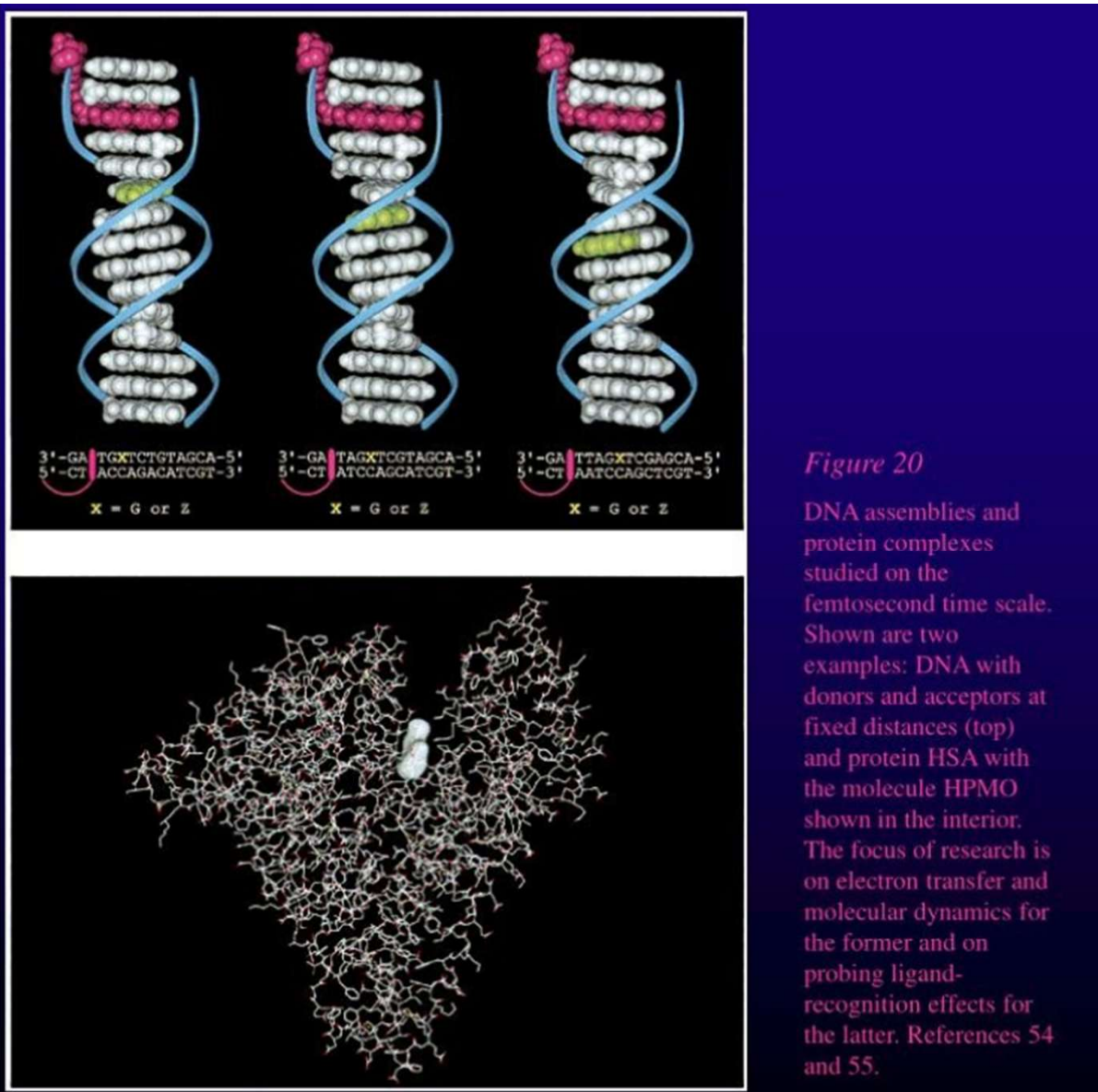


Figure 19

Localized control by femtosecond wave packet preparation at high energies, beating IVR. The series has the same reaction coordinate (C-C bond), but the molecular size has increased in complexity.

Reference 53.



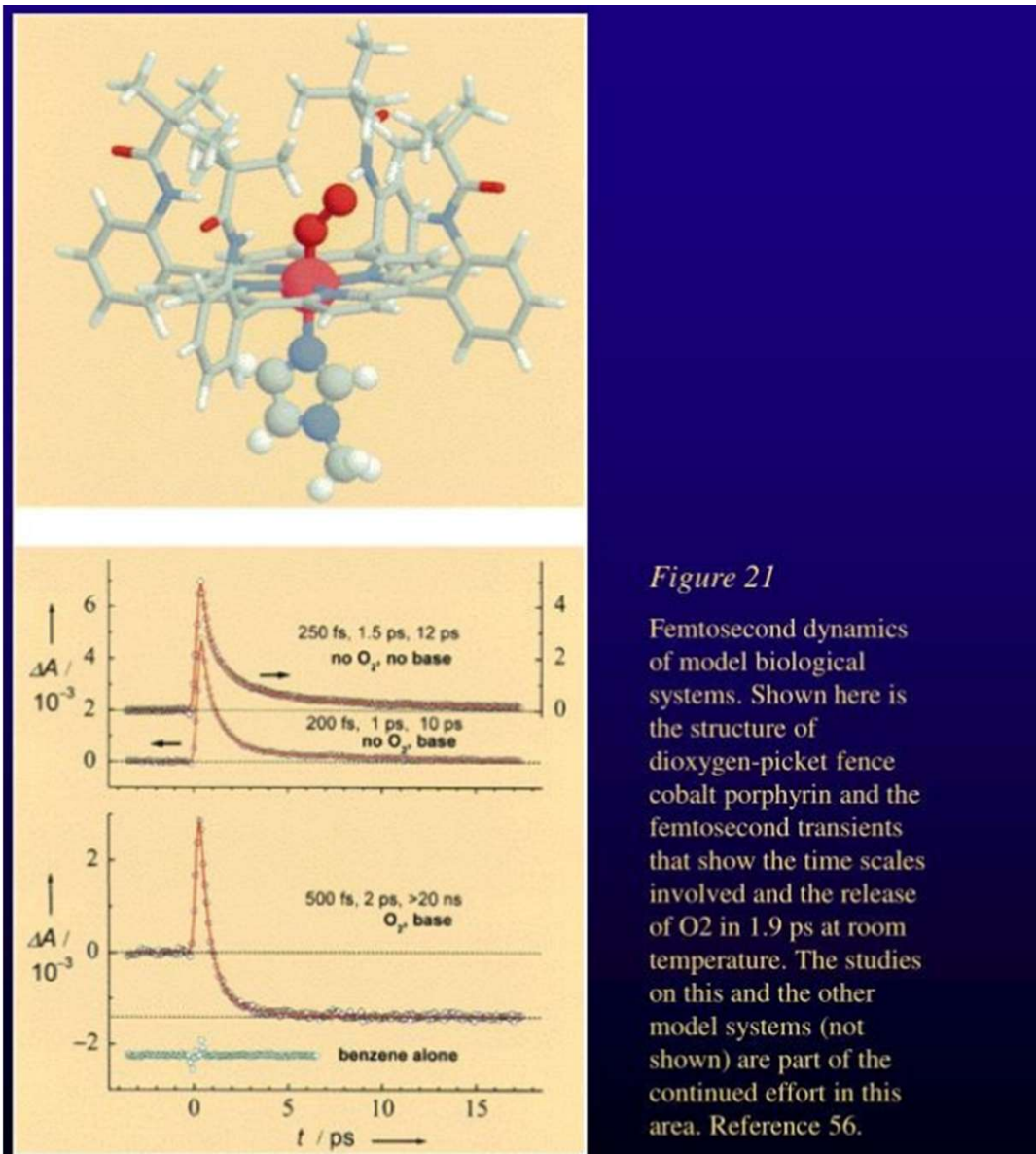


Figure 21
Femtosecond dynamics
of model biological
systems. Shown here is
the structure of
dioxygen-picket fence
cobalt porphyrin and the
femtosecond transients
that show the time scales
involved and the release
of O₂ in 1.9 ps at room
temperature. The studies
on this and the other
model systems (not
shown) are part of the
continued effort in this
area. Reference 56.

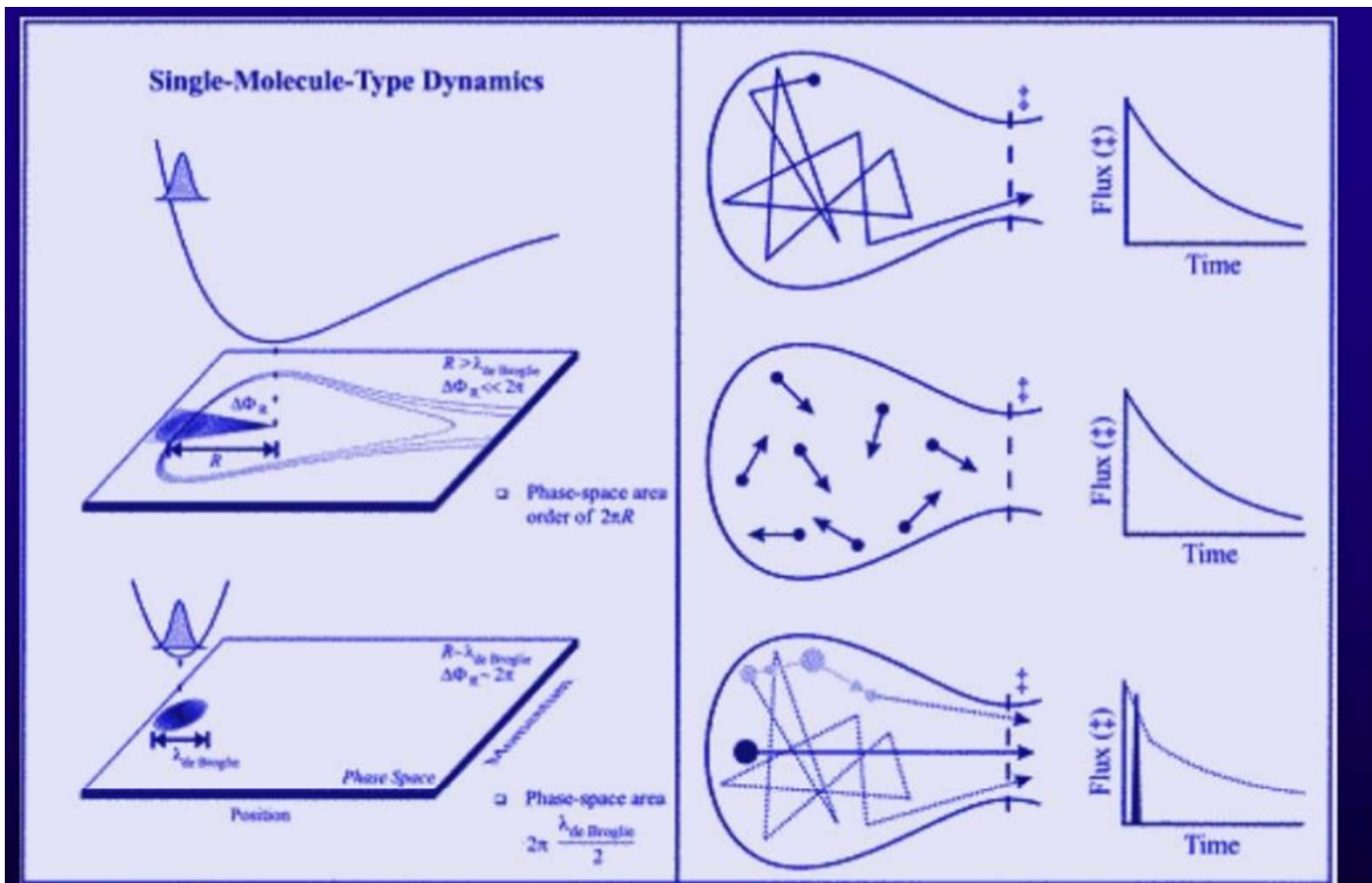


Figure 22 Concept of coherence, both in the dynamics at the atomic scale and in the control of nonstatistical behavior. Shown is the phase space picture, describing the robustness of coherence (left); note the phase-space area of the initial state relative to that of the reaction. (Right) We present, for simplicity, a schematic of a configuration space made of the reactive coordinate and all nonreactive coordinates perpendicular to it (an equivalent phase-space picture can be made). Shown are three cases of interest: (top) the ergodic dynamics, (middle) the incoherent preparation, and (bottom) the coherent wave packet preparation, showing the initial localization, spatially and temporally, and the bifurcation into direct and indirect reaction trajectories. Recent theoretical work (K. Mller, this laboratory) of the corresponding temporal behavior has elucidated the different regimes for the influence of the initial preparation, from a wave packet to a microcanonical limit.

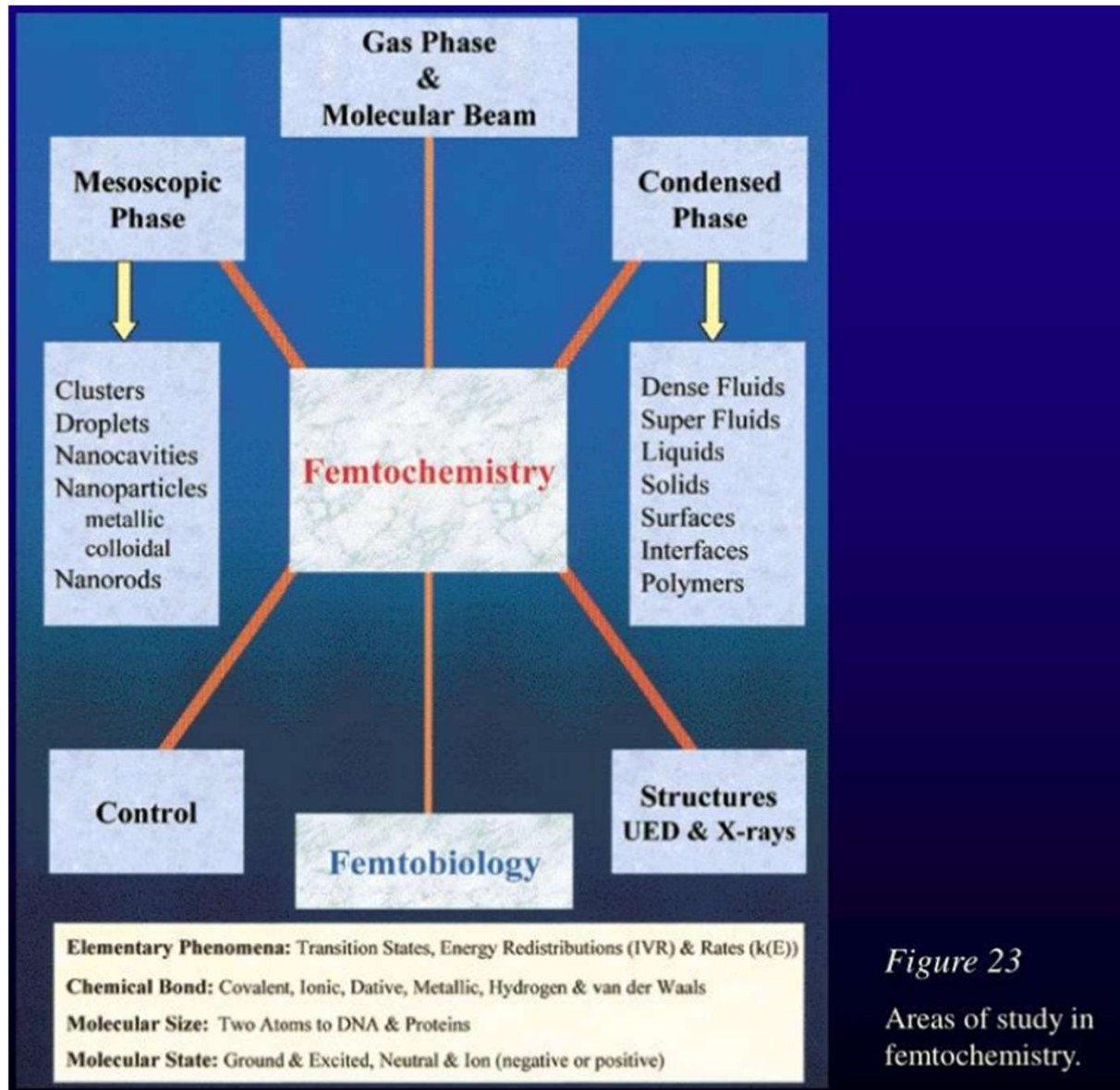
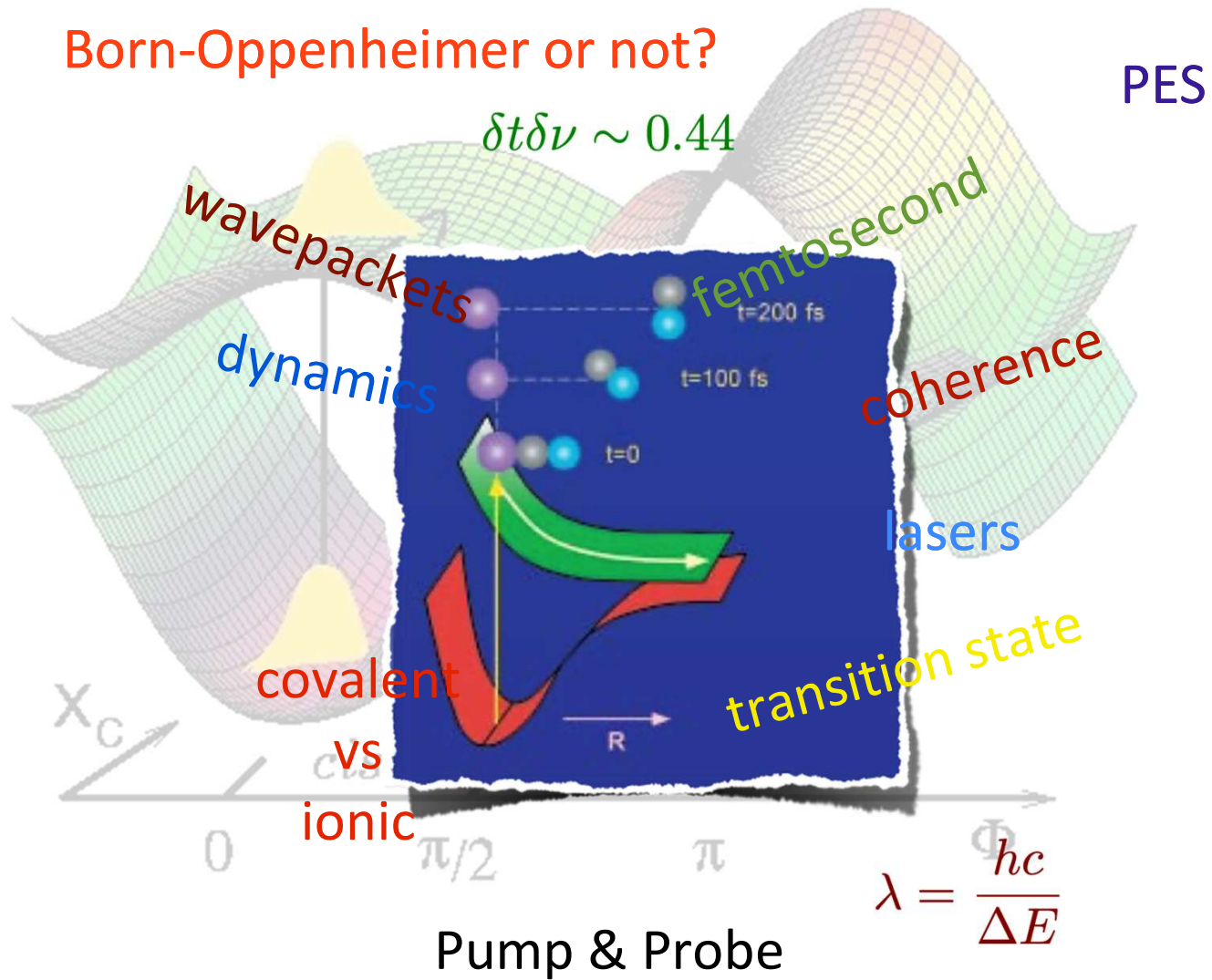


Figure 23
Areas of study in
femtochemistry.

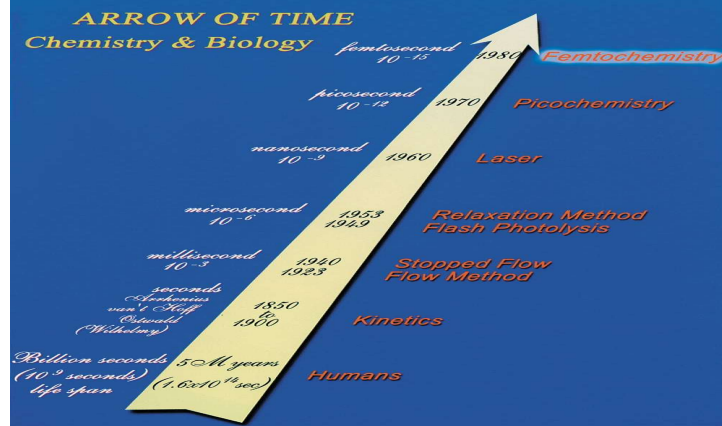
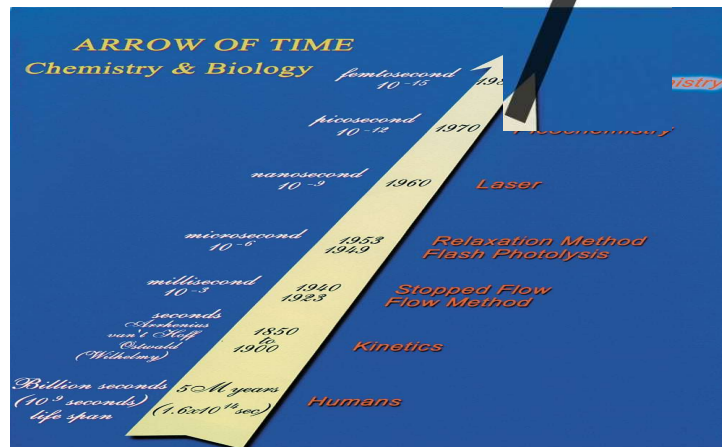
Born-Oppenheimer or not?



unkept promises...

Attosecond
10-18

Attochemistry?



Timescale for
electron motion!

ATTOSECOND SCIENCE

Attoclocks play devil's advocate

An 'attoclock' that measures the relative release time of electrons during double ionization may force us to rethink our use of semi-classical models.

Kiyoshi Ueda and Kenichi L. Ishikawa

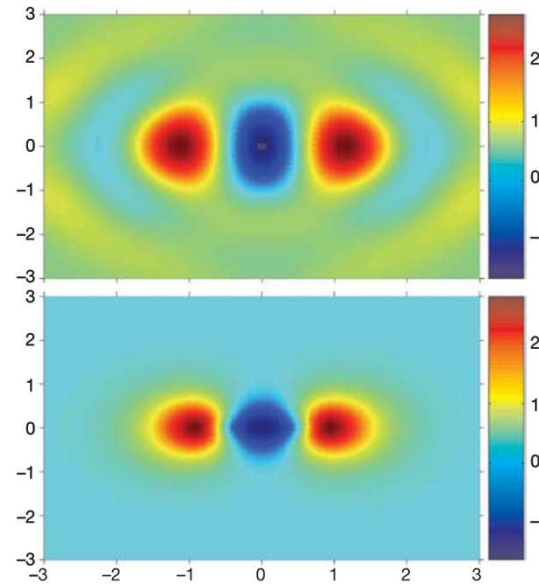
Attosecond science

P. B. Corkum¹ & Ferenc Krausz^{2,3}

The motion of electrons on the atomic scale has been hidden from direct experimental access until recently. We review the revolution in technology that opened the door to real-time observation and time-domain control of atomic-scale electron dynamics, and address the expected implications of having the tools to monitor electrons with subatomic resolution in both space and time.

Tomographic imaging of molecular orbitals

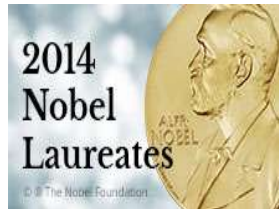
J. Itatani^{1,2}, J. Levesque^{1,3}, D. Zeidler¹, Hiromichi Nilkura^{1,4}, H. Pépin³, J. C. Kieffer³, P. B. Corkum¹ & D. M. Villeneuve¹



Introducing

Module 2:

Super-resolution Microscopy: Development of super-resolved fluorescence microscopy



2014 Chemistry Nobel Prize: Awarded
jointly to **Eric Betzig, Stefan W. Hell**
& William E. Moerner "*for the
development of super-resolved
fluorescence microscopy*"

Taken from:

Debabrata Goswami

Lecture of the Physics Society, Indian Institute of Technology
Kanpur



Eric Betzig

Born: 13 January 1960, Ann Arbor, MI,
USA

Affiliation at the time of the award:
Janelia Research Campus, Howard Hughes
Medical Institute, Ashburn, VA, USA

Prize motivation: "for the development of
super-resolved fluorescence microscopy"

Field: physical chemistry

Prize share: 1/3



Stefan W. Hell



Born: 23 December 1962, Arad, Romania

Affiliation at the time of the award:

Max Planck Institute for Biophysical
Chemistry, Göttingen, Germany, German
Cancer Research Center, Heidelberg,
Germany

Prize motivation: "for the development of
super-resolved fluorescence microscopy"

Field: physical chemistry

Prize share: 1/3





William E. Moerner

Born: 24 June 1953, Pleasanton, CA, USA

Affiliation at the time of the award:

Stanford University, Stanford, CA, USA

Prize motivation: "for the development of super-resolved fluorescence microscopy"

Field: physical chemistry

Prize share: 1/3



Kungliga
Svenska Vetenskapsakademien
har den 8 oktober 2014 beslutat
att med det

NOBELPRIS
som detta år tillerkännes den
som gjort den viktigaste kemiska
upptäckten eller förhållningen
genom samit belöna

William E Moerner
Eric Betzig och Stefan W Hell
för utveckling av superupplöst
fluorescensmikroskopি

STOCKHOLM DEN 10 DECEMBER 2014

Balderam Hoffmann

2014 Chemistry Nobel Lecture details

Single Molecules, Cells, and Super-Resolution Optics

Eric Betzig

Janelia Research Campus, Howard Hughes Medical Institute, Ashburn, VA, USA
8 December 2014 at the Aula Magna, Stockholm University

Nanoscopy with Focused Light

Stefan W. Hell

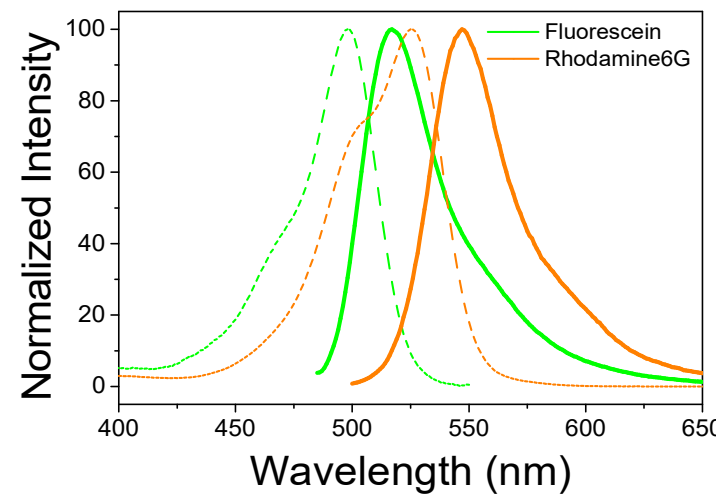
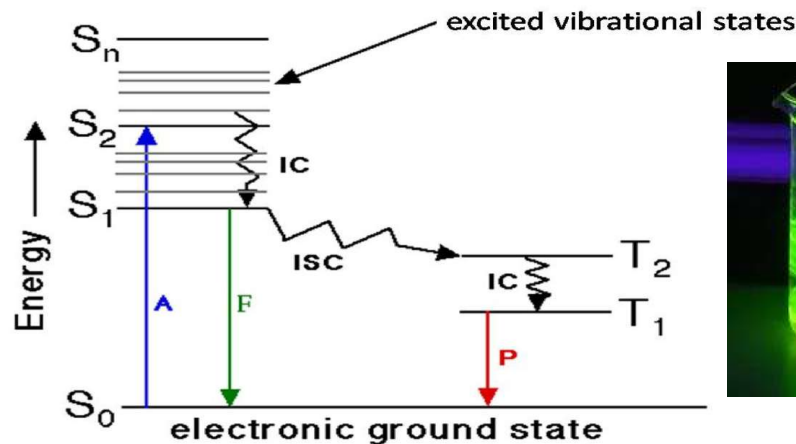
Max Planck Institute for Biophysical Chemistry, Göttingen, and German Cancer
Research Center, Heidelberg, Germany
8 December 2014 at the Aula Magna, Stockholm University.

Single-Molecule Spectroscopy, Imaging, and Photocontrol: Foundations for Super-Resolution Microscopy

William E. Moerner

Stanford University, Stanford, CA, USA
8 December 2014 at the Aula Magna, Stockholm University

What is Fluorescence ?



Stokes Shift of
Fluorescence

Aleksander Jabłoński
1898 – 1980

